Age-Related Changes to the P3a and P3b

Evatte Tiana Sciberras-Lim

A thesis submitted in fulfillment of the requirements for the degree of Doctorate of Philosophy in Psychology , The University of Auckland, 2023.

Preface

The goal of the current thesis was to examine the neural dynamics responsible for the age-related changes to target and distractor processing. Initially we started off with a study using the target-decoy paradigm. However, the technical difficulties involved in modelling the neural dynamics involved in the generation of small lateralised potentials such as the N2pc and Pd encouraged us to employ a different paradigm. The 3-stimulus oddball paradigm stood out as an obvious choice; there was significant evidence that aging affects the generation of the P3a and P3b, and the large size of these components made it possible to model the neural dynamics responsible for the generation of these ERP components. To keep the thesis cohesive, we have only included the work we did using the oddball paradigm, while the other experiment was written up separately. The design of the study allowed us to examine multiple aspects of target and distractor processing in the same group of participants.

Abstract

Over the last 40 years, many studies have shown significant age-related changes to the amplitude, latency and topography of the P3a and P3b (Brown, Marsh, & LaRue, 1983; Fein & Turetsky, 1989; Fjell & Walhovd, 2001; Fjell & Walhovd, 2003; Fjell & Walhovd, 2004; Fjell, Walhovd, & Reinvang, 2005; Fjell & Walhovd, 2005a; Fjell & Walhovd, 2005b; Fjell, Walhovd, Fischl, & Reinvang, 2007; Fjell, Rosquist, & Walhovd, 2009; Walhovd & Fjell, 2003; Walhovd, Rosquist, & Fjell, 2008). In the current thesis we focused on examining the age-related changes to the underlying neural dynamics responsible for the age-related changes to the P3a and P3b. In chapter 2, we perform a wavelet transformation (WT) analysis of the P3a and P3b in younger and older adults to explore the age-related changes to the underlying neurocognitive processes involved in target and distractor processing. In chapter 3, we use dynamic causal modelling (DCM) to examine the network dynamics responsible for the generation of the P3a and P3b, and explore how these dynamics change during the course of healthy aging. In chapter 4, we use two commonly used graph theory metrics to quantify the age-related changes in intrinsic functional connectivity of frontoparietal regions involved the generation of the P3a and P3b.

Acknowledgements

Firstly, I would like to thank my primary supervisor Prof. Tony Lambert for the patience, support and kindness over the last few years. Thank you for giving me the space to explore, and for being so patient when early experiments did not work out. Thank you for being so encouraging when I needed it. Thanks to my secondary supervisor Prof. Paul Corballis, reading your PhD thesis served as the inspiration to keep things nice and concise. Thank you to Veema for making sure all the data collection went smoothly, but also for teaching me everything I know about how to design and run an EEG experiment, and also for just being awesome. Thanks to Jaimie for being an excellent role model. Watching you balance school, work, and raising 2 kids makes me realise I have so much to learn about time management. Thanks to Charissa for absolutely everything, there just isn't enough space to list out everything I'm thankful for. Thanks to J.D. and A.A for all the wonderful advice.

Table of Contents

Preface II
Abstract III
Acknowledgements IV
List of Tables VII
List of Figures VIII
Chapter 1: General Introduction 1
Introduction and Aims 1
The P300 2
Time-Frequency Analysis of the P300 5
Neural Generators of the P3a and P3b 7
Age-related Changes to the P3a and P3b 14
Current Objectives 18
Chapter 2: Wavelet Analysis of the Age-related Changes to the P3a and P3b 19
Methodology 20
Participants 20
Stimuli & Experimental Procedures. 20
EEG Recordings 22
EEG Preprocessing 23
Wavelet transform of ERP data 24
Results 28
Behavioral Results 28
ERP Results 28
ERP Wavelet Analysis Results 31
Discussion 34
Chapter 3: Age-related Changes to the P3a and P3b—A Dynamic Causal Modelling Study 38
Methodology 38
Participants and Data Collection 38
Dynamic Causal Modelling 39
Individual DCM Specification 41
Parametric Empirical Bayes and Bayesian Model Reduction 43
Results 44
DCM Results: P3a (Distractor Oddball) 44
DCM Results: P3b (Target Oddball) 44
Discussion 46
Chapter 4: Relationships between Intrinsic Functional Connectivity and the Age-related Changes to the P3a and P3b 50
Methodology 51
Participants 51

EEG Resting-State Task 51
EEG Recording. 52
Resting-State Data Pre-Processing & Network Analysis. 52
Resting-State Network Properties 54
ERP Data 55
Results 55
Discussion 58
Chapter 5: General Discussion 62
Limitations & Future Directions 65
Conclusion 66
References 68

List of Tables

Table 1. 3-Stimulus oddball task behavioural data 28

Table 2. Correlation between global efficiency and P3a. 57

Table 3. Correlation between global efficiency and P3b. 57

Table 4. Correlation between local efficiency and P3a. 57

Table 5. Correlation between local efficiency and P3b. 57

List of Figures

Figure 1. Schematic illustration of the context updating theory of P300 generation, taken from "Updating P300: An integrative theory of P3a and P3b" , by Polich (2007), Clinical Neurophysiology, 118, 2128-2148.....3

Figure 2. Schematic illustration of the dorsal attention network and the ventral attention network, taken from " A causal role for the right angular gyrus in self-location mediated perspective taking" by De Boer et al. (2020), Scientific Reports, 10; 19229. DOI:10.1038/s41598-020-76235-7 11

Figure 3. Schematic illustration of the 3-stimulus oddball task (Ellipse task on the left and rectangular task on the right) 22

Figure 4. Schematic illustration of the time-frequency decomposition of the EEG data. The application of a five-octave wavelet transform to the data yields five sets of coefficients in the 64-128 Hz (high gamma), 32-64 Hz (gamma), 16-32 Hz (beta), 8-16 Hz (alpha), 4-8 Hz (theta) and 0.1-4 Hz (delta) frequency ranges, such that each octave has the necessary number of coefficients for optimal temporal resolution. 27

Figure 5. Grand average of target, distractor and standard ERPs at Fz, Cz and Pz for younger and older adults.....30

Figure 6. Time-frequency representation of non-target and target ERPs for younger adults. The amplitudes of the wavelet coefficients are encoded in colour. 32

Figure 7. Time-frequency representation of non-target and target ERPs for older adults. The amplitudes of the wavelet coefficients are encoded in color.....33

Figure 8. A diagrammatic representation of the hierarchical neural mass model used to model electrophysiological responses. The state equations embody the connection rules described by Fellerman and Van Essen (1991), and reflect the

dynamics of the source regions. The diagram is adapted from “Dynamic causal modelling of evoked responses in EEG and MEG”, by David et al. (2006), NeuroImage, 30, 1255-1272. 40

Figure 9. Model specification for both P3a and P3b (left). The regions are connected with both feedforward and feedback connections, with broken lines representing the regions that were allowed to be modulated by experimental perturbation. Sources of activity were modelled as dipoles (estimated posterior moments and locations), and are superimposed in an MRI of a standard brain in MNI space (right). 42

Figure 10. The DCM results showing the connections that were significantly modulated by the presentation of distractors (left panel) and the presentation of targets (right panel). The commonalities between younger and older adults are presented in the top panel, while the differences between younger and older adults are represented in the bottom panel. In the top panel, positive posterior parameter estimates indicate an increase in connectivity strength, while negative posterior parameter estimates represent a decrease in connectivity strength between regions. In the bottom panel, positive posterior parameter estimates indicate stronger modulation of connectivity in older adults, while negative posterior parameter estimates indicate weaker modulation of connectivity in older adults relative to younger adults.....45

Figure 11. Global efficiency and (b) Local Efficiency for both older and younger participants. Error bars reflect standard error of the mean. ** = $p < .01$.....56

Chapter 1: General Introduction

Introduction and Aims

Attention refers to the dedication of mental resources either externally towards the processing of a particular sensory input, or internally towards the processing of a particular mental representation (Chun, Golomb, & Turk-Browne, 2011). The dedication of mental resources towards selected items enables us to organize and prioritize information based on their relevance to our current behavioral goals (Chun et al., 2011; Pashler, Johnston, & Ruthruff, 2001; Posner & Petersen, 1990). However, because of our limited resources, and the overwhelming amount of information that is available at any given moment, the ability to rapidly evaluate the potential significance of an unexpectedly presented stimulus is essential for the efficient deployment of attentional resources (Pashler et al., 2001). In the laboratory, the ability to rapidly evaluate and respond to the presentation of an unexpected stimulus is typically examined using the oddball task, and the neural response to the unexpected stimulus is examined by measuring the amplitude and latency of the event-related potential (ERP) component known as the P300 (Linden, 2005; Polich, 2003; Polich, 2007; Sutton, Braren, Zubin, & John, 1965).

Over the years, the P300 has become one of the most extensively studied ERP components (Donchin & Coles, 1988; Johnson Jr, 1989; Johnson Jr, 1993; Kutas, McCarthy, & Donchin, 1977; Polich, 1996; Rugg, Pickles, Potter, & Roberts, 1991). Since the P300 was first reported by Sutton and colleagues in 1965, studies examining the P300 have been conducted to investigate everything from clinical conditions such as schizophrenia (Bramon, Rabe-Hesketh, Sham, Murray, & Frangou, 2004; Jeon & Polich, 2003), and alcoholism (Hesselbrock, Begleiter, Porjesz, O'Connor, & Bauer, 2001;

Polich, Pollock, & Bloom, 1994), to examining age-related cognitive changes (Barrett, Neshige, & Shibasaki, 1987; Friedman, Kazmerski, & Fabiani, 1997; Friedman, 2003; Goodin, Squires, Henderson, & Starr, 1978; Polich, 1997; Rossini, Rossi, Babiloni, & Polich, 2007). The sensitivity of the P300 to neurological changes in psychiatric disorders and aging has sparked significant interest in exploring the neural dynamics involved in the generation of the P300 (Bledowski, Prvulovic, Goebel, Zanella, & Linden, 2004; Bledowski et al., 2004; Bocquillon et al., 2011; Kim, H., 2014; Wood & McCarthy, 1985). In the current thesis, we focus specifically on how these dynamics change during the course of healthy aging.

The P300

The P300 is a positive polarity ERP component that is elicited by the presentation of a stimulus that may be considered deviant due to its temporal or spatial characteristics (Polich, 2003; Polich, 2007; Sutton et al., 1965). According to the context updating theory of P300 generation, the P300 reflects the neural activity associated with the updating of our mental model of the environment caused by the presentation of an unexpected stimulus (Donchin, 1981; Donchin & Coles, 1988). It suggests that after the initial sensory processing of an incoming stimulus is completed, a comparison is made between the newly presented stimulus and the mental template of what we expect to see (i.e. standard stimulus). If no difference is detected, the current mental model of the environment is maintained, and only sensory evoked potentials are recorded (N100, P200, N200). However, if a new stimulus is detected, an ‘‘update’’ of our mental model of our environment occurs and this is reflected by the P300 component (Donchin & Coles, 1988) (see figure 1). The latency of the P300 is hypothesized to reflect how long it takes to detect and evaluate the relevance of the unexpectedly presented stimulus (Magliero, Bashore, Coles, & Donchin, 1984), whilst the magnitude of the P300 component is

proportional to the degree of "surprise" associated with the presentation of the new stimulus (Polich, 2007; Sutton et al., 1965). This means that the amplitude of the P300 component is modulated by any factor that affects the observer's expectations about the likelihood of the stimulus appearance, such as novelty of the stimulus, as well as probability of the stimulus occurrence (Donchin, 1981; Donchin & Coles, 1988; Duncan-Johnson & Donchin, 1977; Goldstein, Spencer, & Donchin, 2002; Pritchard, 1981; Squires, Donchin, Herning, & McCarthy, 1977).

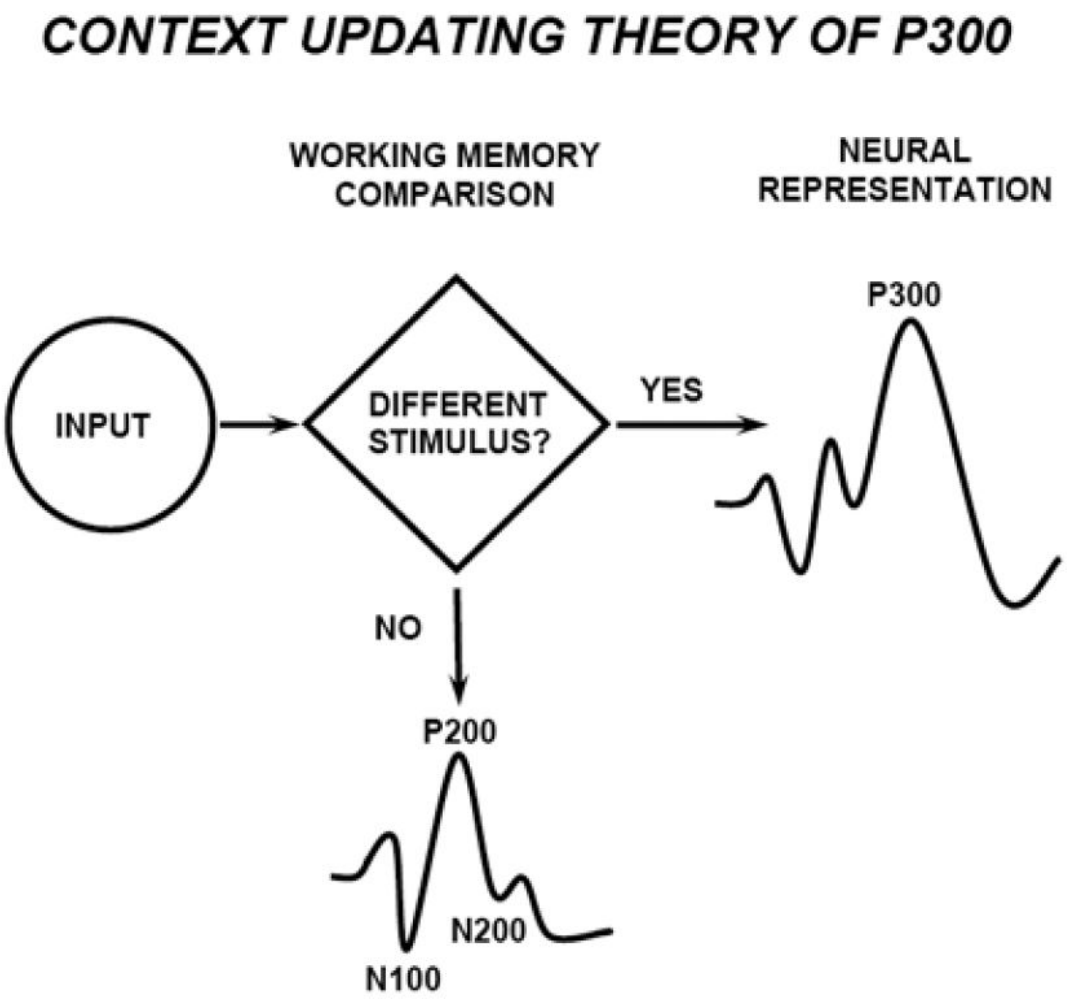

Figure 1. Schematic illustration of the context updating theory of P300 generation, taken from "Updating P300: An integrative theory of P3a and P3b" , by Polich (2007), *Clinical Neurophysiology, 118,* 2128-2148.

In the laboratory, the classical oddball task and the 3-stimulus oddball task are routinely used to assess the impact that stimulus characteristics and stimulus context have on the amplitude, latency, and topography of the P300 component (Polich & Bondurant, 1997; Polich, 2007). In the classical oddball task, participants are required to respond to the presentation of an infrequently presented target stimulus embedded in a string of frequently presented standard stimuli. The presentation of this target stimulus elicits an ERP component referred to as the P3b, which peaks at parietal sites approximately 300-600ms post target stimulus presentation (Comerchero & Polich, 1999; Polich, 2007; Verleger, 2008).

In the 3-stimulus oddball task, another infrequently presented stimulus is inserted into the sequence of target and standard stimuli, these stimuli act as distractors which participants are required to ignore (Courchesne, Hillyard, & Galambos, 1975; Knight, 1996; Knight & Scabini, 1998; Squires, Donchin, Herning, & McCarthy, 1977). The presentation of the distractor stimulus elicits an ERP component referred to as the P3a (Courchesne et al., 1975; Squires et al., 1977). The P3a peaks approximately 250-400ms after the presentation of the distractor stimulus and is maximal at frontocentral sites or centroparietal sites, depending on the type of distractor used (Comerchero & Polich, 1999; Katayama & Polich, 1998). When novel (non-repeated) stimuli are used as distractors, these distractors elicit a P3a that is maximal at frontocentral sites (Courchesne et al., 1975). Conversely, when non-novel distractors are used, these distractors elicit a P3a that is maximal at centroparietal sites (Falkenstein, Hoormann, & Hohnsbein, 1999).

Early attempts to characterize the functional significance of the P3a and P3b suggest that the P3a reflects the bottom-up orienting of attention towards unexpected stimuli (Escera, Alho, Winkler, & Näätänen, 1998; Friedman, Cycowicz, & Gaeta, 2001;

Polich & Criado, 2006; Sawaki & Katayama, 2008), whilst the P3b reflects the top-down allocation of attention for stimulus evaluation or context updating purposes (Donchin, 1981; Donchin & Coles, 1988; Nieuwenhuis, Aston-Jones, & Cohen, 2005; Verleger, 2008). However, subsequent investigations with spatiotemporal principal component analysis and independent component analysis suggests that the P3a and P3b share the same underlying mechanisms (Debener, Makeig, Delorme, & Engel, 2005; Spencer, Dien, & Donchin, 1999; Spencer, Dien, & Donchin, 2001). More specifically, both the P3a and the P3b consist of a frontocentral component as well as a centroparietal component (Spencer et al., 2001). The extent to which each of these components contribute to the scalp-recorded ERPs depends on the stimulus characteristics and the context in which these stimuli are presented, which results in the observed differences between the P3a and P3b (Demiralp, Ademoglu, Comerchero, & Polich, 2001; Spencer et al., 2001; Yordanova, Devrim, Kolev, Ademoglu, & Demiralp, 2000). It is therefore important to not only examine the age-related changes to the amplitude and latency of the P3a and P3b, but also to explore the underlying processes that contribute towards these changes.

Time-Frequency Analysis of the P300

However, despite the fact that EEG signals can provide information about the timing, location, and frequency of various neurocognitive processes, many studies have focused only on analysing these signals in the time domain, by measuring the amplitude and latency of ERPs (Cohen, 2014). The ERP technique has become the normative method for analysing EEG signals due to its computational efficiency, the high temporal precision of the method, and the assumption that each ERP component is uniquely related to a particular neurocognitive process (Luck, Woodman, & Vogel, 2000; Luck, 2014; Woodman, 2010). Even though ERP studies have provided some much-needed insights

into the neural processes that subserve various sensory, perceptual, and cognitive processes, the ERP technique is not without its drawbacks (Gaillard, 1988). Most notably, the ERP technique does not allow us to tease apart neural processes that overlap along both the temporal and spatial dimensions (Bernat, Williams, & Gehring, 2005; Cohen, 2014). On the other hand, because time-frequency analysis allows us to distinguish processes that differ along either the temporal, spatial or frequency dimension, studies employing these techniques permit a more detailed exploration of the underlying neural dynamics involved in attentional processing (Ademoglu, Demiralp, Yordanova, Kolev, & Devrim, 1998; Bachman & Bernat, 2018; Bernat et al., 2005; Daubechies, 1990).

Time-frequency analysis also allows us to index the neurophysiological mechanisms that underlie various cognitive processes because oscillations in the EEG signal directly reflect neuronal oscillations within the cortex, and the underlying mechanisms that generate population-level oscillations are relatively well understood and can be modeled relatively precisely (Buzsáki & Wang, 2012; Cohen, 2014). Furthermore, because neuronal oscillations support brain function across multiple spatial and temporal scales (Cohen, 2014; Murray, Demirtaş, & Anticevic, 2018; Schürmann & Başar, 2001); examining the age-related changes to neuronal oscillations may provide a meaningful avenue for exploring the underlying neurophysiological mechanisms that contribute to the age-related declines to attention that have been documented across behavioural (Healey, Campbell, & Hasher, 2008; Kim, S., Hasher, & Zacks, 2007), electrophysiological (de Fockert, Ramchurn, Van Velzen, Bergström, & Bunce, 2009; Fabiani, Low, Wee, Sable, & Gratton, 2006; Sciberras-Lim & Lambert, 2017) and neuroimaging studies (Campbell, Grady, Ng, & Hasher, 2012; Schmitz, Cheng, & De Rosa, 2010).

Typically, time-frequency analyses have focused on examining activity within the canonical frequency bands: alpha (8-13 Hz), beta (13-30 Hz), gamma (30-70 Hz), delta (0-3 Hz), and theta (3-7Hz) (Cohen, 2014). Substantial evidence has implicated activity within these frequency bands to a variety of sensorimotor and cognitive processes (Başar, Başar-Eroglu, Karakaş, & Schürmann, 2001). For instance, alpha-band activity has been implicated in top-down attention and memory processes (Başar & Güntekin, 2012; Clayton, Yeung, & Kadosh, 2015; Olga, 2012), whilst beta-band activity has been linked to sensorimotor functions and decision-making processes (Palmer, C., Zapparoli, & Kilner, 2016; Schmidt et al., 2019; Spitzer & Haegens, 2017). More importantly, several studies suggests that activity within the delta- and theta-bands can account for the majority of the variance in the P3a and P3b (Başar-Eroglu, Başar, Demiralp, & Schürmann, 1992; Kolev, Demiralp, Yordanova, Ademoglu, & Isoglu-Alkaç, 1997; Yordanova et al., 2000). These studies show that the P3a and P3b consists of theta-band activity in the frontocentral areas, and delta-band activity in centroparietal areas (Bachman & Bernat, 2018; Demiralp et al., 2001; Harper, Malone, & Iacono, 2017). The frontocentral theta-band activity is hypothesized to reflect the orienting of attention to the novel or unexpected stimulus (Demiralp et al., 2001; Harper et al., 2017), whilst the centroparietal delta-band activity has been associated with the stimulus evaluation process that determines if the current stimulus matches our mental template of what we expect to see (Demiralp et al., 2001).

Neural Generators of the P3a and P3b

Due to the utility of the P3a and P3b as potential biomarkers for neurodegenerative diseases (Filipović & Kostić, 1995; Hedges et al., 2016; Rossini et al., 2007), there has also been a significant amount of interest in identifying the neural generators responsible for the generation of these components (Bledowski et al., 2004;

Bledowski et al., 2004; Clark, Fannon, Lai, Benson, & Bauer, 2000; Halgren, Baudena, Clarke, Heit, Marinkovic et al., 1995; Halgren et al., 1995a; Smith et al., 1990; Volpe et al., 2007). However, the results have been somewhat inconsistent across studies (Bocquillon et al., 2011; Kim, H., 2014; Linden, 2005). As a result, Linden (2005) proposed that a region should only be considered a neural generator for the P3a/P3b if there was converging evidence from at least two techniques to suggests that it contributes to the generation of these components.

Early efforts to localize the neural generators responsible for the generation of the P3a and P3b relied on the use of intracranial recordings of the P300 in those with intractable epilepsy (Baudena, Halgren, Heit, & Clarke, 1995; Halgren et al., 1995a; Halgren et al., 1995b; Smith et al., 1990). The results from these studies suggests that the generation of the P3b involves the activation of the prefrontal cortex (Wood & McCarthy, 1985), inferior parietal cortex (Smith et al., 1990), superior parietal cortex (Halgren et al., 1995a), temporal cortex (Halgren et al., 1995b), and the anterior cingulate cortex (Smith et al., 1990; Wang, Ulbert, Schomer, Marinkovic, & Halgren, 2005); while generation of the P3a involves the activation of the inferior parietal lobe/supramarginal gyrus, superior temporal sulcus (Halgren et al., 1995; Halgren et al., 1995b), dorsolateral and orbital frontal cortices, as well as, the anterior cingulate cortex (Baudena et al., 1995). However, although the use of intracerebral recordings was a promising early step towards localizing the neural generators responsible for the generation of the P3a and the P3b, the use of intracerebral recordings suffers from several limitations. Firstly, the small number of implanted electrodes makes it hard to localize the generators of intracranial potentials with a high degree of accuracy (Koessler et al., 2015; Lachaux, Rudrauf, & Kahane, 2003; Parvizi & Kastner, 2018). Secondly, because the placement of electrodes is determined by clinical needs the electrodes may not be ideally located to measure the

intracranial correlates of the P3a and P3b (Lachaux et al., 2003; Parvizi & Kastner, 2018). Lastly, the interictal firing patterns in epileptic patients might also differ from the neuronal firing patterns of healthy adults (Lachaux et al., 2003; Parvizi & Kastner, 2018).

Additionally, while intracerebral recordings suggest a distributed network of regions are involved in the generation of the P3a and P3b, lesion studies suggest that not all these regions are crucial for the generation of the P3a and P3b. Instead, lesion studies suggest that the most significant amplitude reductions to the P3a are caused by lesions to frontal cortical regions (Daffner et al., 2000; Knight, 1984; Knight & Scabini, 1998), although lesions to the temporal, and parietal sites also cause significant attenuation of the P3a (Knight & Scabini, 1998; Linden, 2005). In contrast, the P3b is most significantly affected by lesions to the tempoparietal junction (Knight, Scabini, Woods, & Clayworth, 1989; Verleger, 1988), while lesions to other sites appear to have little impact on the amplitude and latency of the P3b (Johnson Jr, 1989; Polich & Squire, 1993). However, interpreting the results from lesion studies is not without its own set of challenges. For instance, because focal lesions caused by illness, injury or neurosurgery are not under experimental control, they may vary in the extent of damage caused (Rorden & Karnath, 2004; Vaidya, Pujara, Petrides, Murray, & Fellows, 2019), which makes it more challenging to establish a relationship between a given lesion and the consequent behavioral deficits (Vaidya et al., 2019). Furthermore, individuals may experience a period of more pronounced behavioral deficits immediately following a brain injury which may subsequently abate due to the functional reorganization of neural networks (Vaidya et al., 2019; Wieloch & Nikolich, 2006). Moreover, the etiology of a lesion may also affect how the brain adapts to damage (Cipolotti et al., 2015). For example, functional changes following brain injury as a result of stroke are most severe immediately after the stroke, with some recovery of function occurring in the months

following the stroke (Jørgensen et al., 1995; Verheyden et al., 2008). On the other hand, brain tumors cause damage over a more extended period of time, through compression, distortion, or through edemas, and changes to microcircutry (Desmurget, Bonnetblanc, & Duffau, 2007; Duffau, 2011; Esquenazi, Lo, & Lee, 2017; Shallice, Mussoni, D'Agostino, & Skrap, 2010). This complicates our ability to draw firm conclusions about the involvement of a given region in the generation of the P3a and P3b on the basis of lesions studies alone.

In recent years, the development of electroencephalographic (EEG) source localization techniques, as well as, the increased accessibility of neuroimaging equipment in research institutes around the world has significantly contributed towards attempts to localize the neural generators responsible for the generation of the P3a and the P3b (Bledowski et al., 2004; Bocquillon et al., 2011; Kim, H., 2014; Volpe et al., 2007). These studies have identified two distinct but partially overlapping networks responsible for attentional control (Corbetta & Shulman, 2002; Corbetta, Patel, & Shulman, 2008; Vossel, Weidner, Driver, Friston, & Fink, 2012; Vossel, Geng, & Fink, 2014) (see figure 2). The first network is a bilaterally organized network referred to as the dorsal attention network (DAN), which encompasses the dorsolateral prefrontal cortex (DLPFC), frontal eye fields (FEF), inferior frontal junction (IFJ), intraparietal sulcus (IPS), and motion-sensitive middle temporal area (MT+) (Bressler, Tang, Sylvester, Shulman, & Corbetta, 2008; Corbetta & Shulman, 2002; Corbetta et al., 2008; Kincade, Abrams, Astafiev, Shulman, & Corbetta, 2005; Vossel et al., 2012; Vossel et al., 2014). The second network is a right-lateralized network referred to as the ventral attentional network (VAN), which comprises the temporoparietal junction (TPJ), anterior insula (AI), frontal operculum (FO), and anterior cingulate cortex (ACC) (Corbetta et al., 2008; Fox, Corbetta, Snyder, Vincent, & Raichle, 2006; Vossel et al., 2012; Vossel et al., 2014). These two networks

converge upon the middle frontal gyrus, which serves as a hub facilitating the exchange of information across these networks (Corbetta et al., 2008; Fox et al., 2006; Vossel et al., 2014). Additionally, subdivisions of the superior longitudinal fasciculus (SLF) connect regions within and between these two networks allowing for the efficient transmission of information (De Schotten et al., 2011; Schurr, Zelman, & Mezer, 2020). Specifically, the SLF I connects dorsal frontoparietal areas and the SLF III connects ventral frontoparietal regions, while the SLF II connects the parietal component of the ventral network with the prefrontal component of the dorsal network and is proposed to serve as a crucial communication pathway for the two systems (De Schotten et al., 2011; Schurr et al., 2020). The strong interconnectivity of these networks enables them to work interactively to guide the deployment of attentional resources across the visual field (Corbetta et al., 2008; DiQuattro & Geng, 2011; Vossel et al., 2012; Vossel et al., 2014; Wen, Yao, Liu, & Ding, 2012).

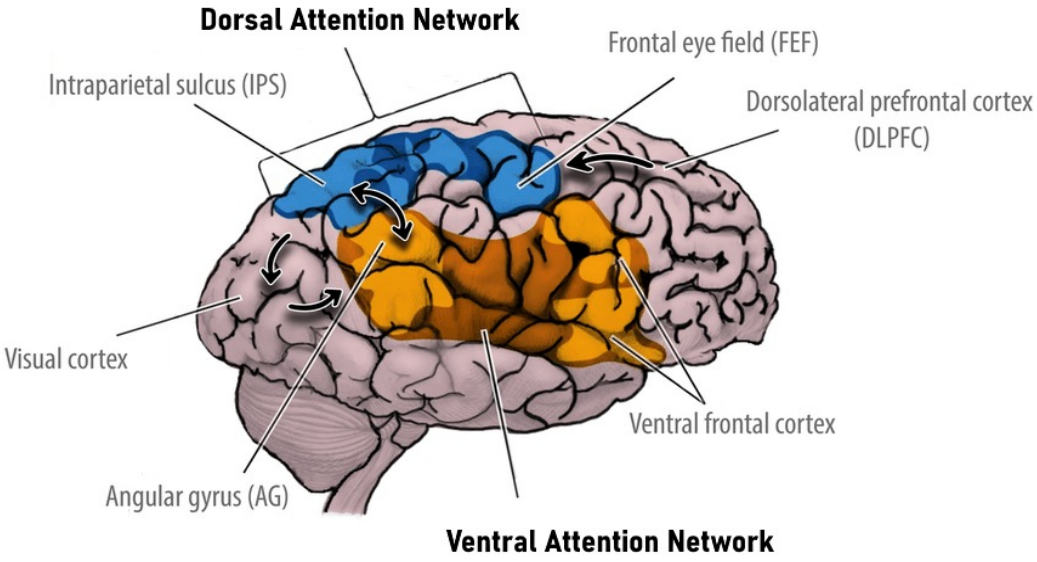

Figure 2. Schematic illustration of the dorsal attention network and the ventral attention network, taken from " A causal role for the right angular gyrus in self-location mediated perspective taking" by De Boer et al. (2020), *Scientific Reports, 10; 19229*. DOI:10.1038/s41598-020-76235-7

Over the years, many studies have been conducted to examine exactly how the DAN and VAN contribute towards the generation of the P3a and P3b (Ardekani et al., 2002; Bledowski et al., 2004; Bocquillon et al., 2011; He, Lian, Spencer, Dien, & Donchin, 2001; Kiehl, Laurens, Duty, Forster, & Liddle, 2001; Kim, H., 2014; Linden et al., 1999; Mulert et al., 2004; Volpe et al., 2007; Yamazaki, Kamijo, Kiyuna, Takaki, & Kuroiwa, 2001). The results from 75 of these studies have been synthesized in a meta-analysis conducted by Kim (2014). The results from the meta-analysis revealed that several VAN regions including AI, IPL, and ACC contribute to the generation of both the P3a and the P3b (Bledowski et al., 2004; Bocquillon et al., 2011; Clark et al., 2000; Kiehl et al., 2001; Mulert et al., 2004; Volpe et al., 2007). These results are consistent with the networks' proposed role in detecting salient environmental changes (Corbetta & Shulman, 2002; Corbetta et al., 2008; Vossel et al., 2012). Several of these studies have also showed that there is more extensive activation in response to targets compared to distractors (Bledowski et al., 2004; Bocquillon et al., 2011). This suggests that VAN activity is not only modulated by stimulus saliency but rather reflects the dynamic interplay between stimulus saliency and individual goals in influencing the deployment of attentional resources (DiQuattro & Geng, 2011; Downar, Crawley, Mikulis, & Davis, 2001; Kim, H., 2014). This is supported by other studies which suggest that although the VAN responds consistently to salient stimuli under passive conditions (Downar, Crawley, Mikulis, & Davis, 2000), the activation of the VAN in response to salient or unexpected items while performing attentionally demanding tasks are contingent upon whether or not these stimuli are behaviourally relevant (Arrington, Carr, Mayer, & Rao, 2000; Corbetta et al., 2008; Downar et al., 2001; Indovina & Macaluso, 2007; Kincade et al., 2005). It is hypothesized that inhibiting the response of VAN structures to salient but

irrelevant items prevents shifts of attention that could negatively interfere with successful task performance (DiQuattro & Geng, 2011; Shulman, Astafiev, McAvoy, d'Avossa, & Corbetta, 2007; Wen et al., 2012).

The results from the Kim (2014) meta-analysis also reveal that there is little consistency across studies concerning the DAN's contribution to the generation of the P3a or P3b. This lack of consistency may be due to several factors. Firstly, because both standard and oddball stimulus processing involves externally directed attention, DAN structures may not be significantly more active in response to oddball stimuli compared to standard stimuli (Kim, H., 2014). Secondly, because feature-based attentional control may involve less extensive subregions of the DAN than space-based attentional control does, oddball stimuli that differ from standard stimuli due to minute featural differences might elicit less widespread activity within the DAN (Giesbrecht, Woldorff, Song, & Mangun, 2003; Liu, Slotnick, Serences, & Yantis, 2003; Serences, Schwarzbach, Courtney, Golay, & Yantis, 2004). Thirdly, because the meta-analysis includes many procedurally different studies and different features activate distinct regions of the DAN (Giesbrecht et al., 2003; Liu et al., 2003; Serences et al., 2004), the results from the meta-analysis may be less sensitive to the DAN's role in oddball processing (Kim, H., 2014). This possibility is consistent with the findings from Kim (2014) which show that the IPS and MT+ are consistently activated during visual oddball studies but not in auditory oddball tasks. Additionally, many studies have highlighted that several key regions of the DAN including the dorsal frontal and parietal regions are indeed involved in the generation of both the P3a and P3b (Bocquillon et al., 2011; Mantini, Corbetta, Perrucci, Romani, & Del Gratta, 2009; Strobel et al., 2008). The DAN is important for the disengagement of attentional resources from the repeatedly presented standard stimuli and the reallocation of attentional resources to the oddball stimuli. The disengagement and

redeployment of attentional resources to these oddball stimuli plays a key role in the successful identification of target stimuli (Bocquillon et al., 2011).

Age-related Changes to the P3a and P3b

As we age, structural deterioration of these large-scale neural networks hinder their ability to function effectively (Bennett & Madden, 2014; Madden et al., 2007; Madden et al., 2012; O'Sullivan et al., 2001; Pfefferbaum et al., 2000). Consequently, older adults exhibit significant age-related decrease in the amplitude of both the P3a and P3b (Fjell & Walhovd, 2004; Fjell, Walhovd, Fischl, & Reinvang, 2007; O'Connell et al., 2012; Walhovd, Rosquist, & Fjell, 2008), as well as, an age-related delay in the latency of the P3a and P3b (Fjell, Rosquist, & Walhovd, 2009; Goodin et al., 1978; Polich, 1996; Polich, 1997). The reduction in the amplitude of these components has been hypothesized to reflect a reduction in the amount of neural resources available for the processing of these oddball stimuli (Fjell & Walhovd, 2001; Walhovd & Fjell, 2003), whilst the latency delays have been proposed to reflect the age-related slowing of stimulus evaluation or context updating processes (Magliero et al., 1984; Polich, 1996; Verleger, Neukäter, Kömpf, & Vieregge, 1991).

There is some evidence to suggest that the P3a may be more sensitive to age-related changes than the P3b (Fjell & Walhovd, 2004). The increased vulnerability of the P3a component is due to the fact that the frontal cortical regions responsible for the generation of the P3a experience significantly more grey matter atrophy and white matter degeneration compared to more posterior regions of the brain (Raz, 2000; Raz et al., 2005). Additionally, PFC function in older adults is also negatively impacted by the decreases in dopamine concentration, dopamine receptor density, and transporter availability, with estimates suggesting that D2 receptor loss may be as high as 13% per decade in the anterior cingulate cortex and 11% per decade in the frontal cortex after the

age of 60 (Bäckman, Nyberg, Lindenberger, Li, & Farde, 2006; Bäckman, Lindenberger, Li, & Nyberg, 2010; Kaasinen et al., 2000; Volkow et al., 2000). Due to the importance of these regions for the generation of the P3a, it has been proposed that decreases in dopamine availability within the PFC significantly contribute towards the age-related declines to the P3a (Bäckman et al., 2006; Bäckman et al., 2010; Braver & Barch, 2002).

In addition to the age-related changes to amplitude and latency of the P3a and P3b, numerous studies have also noted a significant anterior shift in the topography of both the P3a and P3b components (Fabiani, Friedman, & Cheng, 1998; Fjell, Walhovd, & Reinvang, 2005; Friedman et al., 1997; O'Connell et al., 2012). Unfortunately, the functional significance of these shifts remains unclear. Does the anterior shift of these components simply reflect the consequences of frontal lobe deterioration or does it represent an adaptive response to neural declines?

The first proposal suggests that the anterior shift of these components simply reflects a failure to habituate to the novelty of the oddball stimuli (Richardson, Bucks, & Hogan, 2011; West, Schwarb, & Johnson, 2010). According to this proposal, older adults are unable to establish a strong mental representation of target and distractor stimuli, which results in them continuing to exhibit a strong novelty response even after repeated presentations of these oddball stimuli (West et al., 2010). In contrast, young adults are able to quickly establish a strong mental representation of target and distractor stimuli, which facilitates the rapid habituation of the novelty response (Richardson et al., 2011; West et al., 2010). There is evidence that this failure to habituate to the novelty of oddball stimuli may be caused by declines to the frontal cortical regions responsible for executive processing (Fabiani et al., 1998; Lorenzo-López, Amenedo, Pazo-Álvarez, & Cadaveira, 2007; West et al., 2010). For instance, several studies have shown that only older adults with reduced frontal lobe function (Fabiani et al., 1998), or low executive capacity

(West et al., 2010) exhibit an anterior shift to these components. However, this finding has not been universal with several studies finding either no difference in neuropsychological test scores between older adults who exhibit the anterior shift versus those that do not, and studies that show that older adults with higher neuropsychological test scores show a larger anterior shift (Alperin, Mott, Rentz, Holcomb, & Daffner, 2014; Daffner et al., 2006; Riis et al., 2008).

The second proposal suggests that the anterior shift of these components represents an increased reliance on frontally-mediated control mechanisms to support task performance. This proposal stems from the fact that the anterior shift of these components is similar to the increased recruitment of prefrontal regions and reduced activity of posterior cortical regions that older subjects demonstrate on a variety of attentionally demanding tasks (Cabeza, Anderson, Locantore, & McIntosh, 2002; Davis, Dennis, Daselaar, Fleck, & Cabeza, 2008; Lorenzo-López, Amenedo, Pascual-Marqui, & Cadaveira, 2008; Madden, Whiting, Cabeza, & Huettel, 2004; Vallesi, Stuss, McIntosh, & Picton, 2009). For example, a fusion EEG/fMRI study conducted by O'Connell et al. (2012) showed that the anterior shift of these components is caused by increased activation of the frontal and temporal regions and reduced activity in the inferior parietal lobe in older adults. More specifically, it showed that the anterior shift of the P3a was due to increased activation in the left inferior frontal cortex, right cingulate cortex, and the cerebellar vermis, and decreased activity in the right inferior parietal cortex in older relative to younger adults. In a similar vein, the study demonstrated that the anterior shift of the P3b was due to increased activation of the right dorsolateral prefrontal cortex, left superior temporal cortex, left temporal pole, right hippocampus, and left cerebellum in older relative to younger adults. Additionally, since the behavioral performance of older adults in the oddball task is typically comparable to that of younger adults, the anterior

shift of these components has been proposed to reflect the compensatory activation of prefrontal regions to compensate for the reduced activity in posterior cortical regions caused by age-related sensory declines (Davis et al., 2008; O'Connell et al., 2012). (Fabiani et al., 1998; Friedman, Simpson, & Hamberger, 1993; Friedman et al., 1997; Richardson et al., 2011; West et al., 2010).

More recently, studies have also begun to examine how the age-related changes to both brain structural characteristics and functional activity patterns impact the P3a and P3b (Fjell et al., 2005; Fjell et al., 2007; O'Connell et al., 2012). In fact, since Goodin and colleagues' (1978) seminal paper exploring the age-related changes to the P300 component, countless studies have been conducted to explore the causal mechanisms underlying the age-related changes to the P3a and P3b (Fjell et al., 2005; Fjell et al., 2007; O'Connell et al., 2012; Walhovd & Fjell, 2003). For example, a study was conducted by Fjell et al. (2007) to explore how the age-related changes to the amplitude and latency of the P3a and P3b were influenced by age-related changes in cortical volume. The results suggest that in older adults P3a amplitude was positively correlated with the volume of pre- and post-central gyri in both hemispheres, the paracentral gyrus and the inferior frontal gyrus in the right hemisphere, as well as, the middle frontal gyrus, posterior cingulate cortex, and the subcentral gyrus in the left hemisphere. In contrast to the P3a, there was no significant correlation between P3b amplitude and cortical volume. There was however, evidence that P3b latency was negatively correlated with the cortical volume of the insula, subcallosal gyrus, anterior cingulate cortex, superior frontal gyrus, temporal gyrus, and temporal pole. These results suggests that age-related volumetric declines play an important role in age-related changes to target and distractor processing, presumably because regions with a thicker cortex are able to facilitate more efficient

processing of oddball stimuli due to the larger number of neurons and synaptic connections within these regions (Fjell et al., 2007; Pakkenberg & Gundersen, 1997).

Current Objectives

From the above studies, it is clear that many studies have moved beyond simply describing the age-related changes to the P3a and P3b, to actively exploring the functional significance of these changes, as well as identifying the causal mechanisms responsible for these changes. In the current thesis we focus on the age-related changes to the underlying neural dynamics responsible for the age-related changes to the P3a and P3b. In chapter 2, we perform a wavelet transformation (WT) analysis of the P3a and P3b in younger and older adults to explore the age-related changes to the underlying neurocognitive processes involved in target and distractor processing. In chapter 3, we use dynamic causal modelling (DCM) to examine the network dynamics responsible for the generation of the P3a and P3b, and explore how these dynamics change during the course of healthy aging. In chapter 4, we use two commonly used graph theory metrics to quantify the age-related changes in intrinsic functional connectivity of frontoparietal regions involved the generation of the P3a and P3b.

Chapter 2: Wavelet Analysis of the Age-related Changes to the P3a and P3b

Age-related changes to the amplitude and latency of both the P3a and P3b are well-documented in the cognitive aging literature (Fjell et al., 2007; O'Connell et al., 2012; Walhovd & Fjell, 2003; Walhovd et al., 2008). However, because oddball processing involves both the initial orienting of attention towards the unexpectedly presented oddball stimulus, as well as the subsequent evaluation of the significance of the oddball stimulus, the extent to which the age-related changes to the P3a and P3b reflect changes to attentional orienting or stimulus evaluation/context updating processes remains unclear.

Fortunately, time-frequency analysis allows us to tease apart the underlying neurocognitive processes that contribute towards the generation of these ERP components and enables us to examine how they change as we grow older (Cohen, 2014). Previous studies utilising this technique have shown that activity within the delta- and theta-bands can account for the majority of the variance in the P3a and P3b (Başar-Eroglu et al., 1992; Kolev et al., 1997; Yordanova et al., 2000). These studies show that the P3a and P3b consists of theta-band activity in the frontocentral areas, and delta-band activity in centroparietal areas (Bachman & Bernat, 2018; Demiralp et al., 2001; Harper et al., 2017). The frontocentral theta-band activity is hypothesized to reflect the orienting of attention to the novel or unexpected stimulus (Demiralp et al., 2001; Harper et al., 2017), whilst the centroparietal delta-band activity has been associated with the stimulus evaluation process that determines if the current stimulus matches the previous stimulus held in working memory (Demiralp et al., 2001). Therefore, in the current chapter, we used a time-frequency analysis technique known as the continuous wavelet transform (CWT) to examine the age-related changes to the activity within these frequency bands,

in order to determine how the age-related changes to each of these neurocognitive processes contributes towards the age-related changes to the P3a and P3b.

Methodology

Participants

25 young adults (13 males) between the ages of 18-35 (M= 25.12, SD= 4.33) and 25 older adults (4 males) between the ages of 60-85 (M= 73.04, SD= 4.48) were recruited to participate in the experiment, which was approved by the University of Auckland Human Participants Ethics Committee. All participants had corrected-to-normal vision, and reported no prior history of neurological or psychiatric impairment. Additionally, older adults were screened using the Mini-Mental State Examination (MMSE) from The Hartford Institute for Geriatric Nursing, Division of Nursing, New York University (Folstein, Robins, & Helzer, 1983), to ensure that they were free of any cognitive impairments that would significantly impair their ability to understand the instructions provided, or impair their ability to perform the task. The MMSE is an 11- item questionnaire measure, that tests five areas of cognitive function, including 1) orientation, 2) registration, 3) attention and calculation, 4) recall, and 5) language. The approximate time taken to complete the screening was around 5-7 minutes. The maximum score attainable is 30, and participants with a score of 25 and above are considered to be free of significant cognitive impairment. All participants scored above 28 suggesting that they did not have any significant cognitive impairments that would interfere with their ability to perform the task.

Stimuli & Experimental Procedures.

Experimental scripts were created in Matlab (The MathWorks, Inc., Natick, Ma, USA), using the Psychophysics Toolbox extension (Brainard & Vision, 1997; Kleiner, Brainard, & Pelli, 2007). Stimuli were presented on a Samsung Syncmaster 24-inch

screen (Refresh rate: 75Hz; screen resolution: 1920 x 1080 pixels), and participants used a chin rest so they viewed the display from a distance of 57cm. ERPs were recorded while participants performed a visual 3-stimulus oddball paradigm similar to the one utilized in Bledwoski et al. (2004) and Bocquillon et al. (2011). However, the size of the stimuli was modified to match previous studies examining the age-related changes to the P3a and P3b (Fjell & Walhovd, 2004; Fjell et al., 2009; Juckel et al., 2012; Polich, 1996).

After screening, participants first went through the resting-state block described in Chapter 4 prior to the start of the 3-stimulus oddball task. The 3-stimulus oddball tasks consisted of four blocks of trials, with 200 trials per block. As shown in Figure 3, each individual block contained 176 standards (88% of trials), 12 targets (6% of trials), and 12 distractors (6% of trials), presented in pseudorandom order. The presentation of each target or distractor was preceded by between 2-9 standard stimuli, which helped to maximize the temporal interval between successive presentations of oddball stimuli while still ensuring that participants would not be able to predict the upcoming stimulus. Each stimulus was presented on screen for 500ms and the interstimulus interval varied between 1300-1700ms. Participants were told to press the spacebar key whenever they saw the target and to do nothing when the standards and distractors were presented. In two of the blocks, the standard stimulus was a blue ellipse measuring 9° × 7°, the target was a blue ellipse measuring 10° × 8°, and the distractor was a blue rectangle measuring 12° × 10° (ellipse task). In the other two blocks, the standard stimulus was a blue rectangle measuring 9° × 7°, the target was a blue rectangle measuring 10° × 8°, and the distractor was a blue ellipse measuring 12° × 10° (rectangle task). The task order was counterbalanced across participants so that half of the participants performed the ellipse task first while the other half performed the rectangle task first. Before each task,

participants performed a practice round that consisted of nine standard stimuli and two target stimuli before the EEG recording was started.

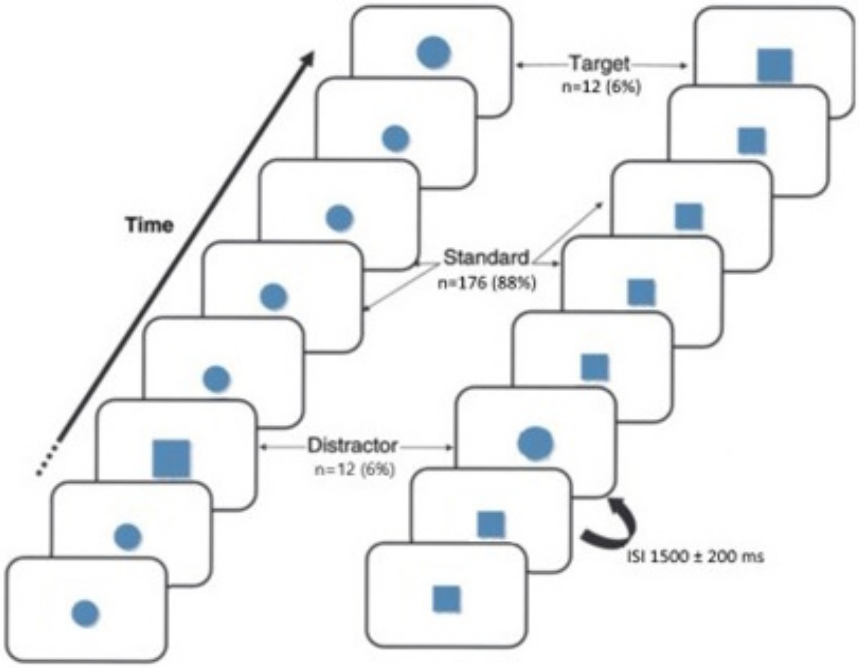

Figure 3. Schematic illustration of the 3-stimulus oddball task (Ellipse task on the left and rectangular task on the right)

EEG Recordings

The electroencephalography (EEG) recordings were conducted in an electrically shielded room (IAC Noise Lock Acoustic - Model 1375, Hampshire, United Kingdom) using 128-channel Ag/AgCl electrode nets (Tucker, 1993) from Electrical Geodesics Inc., (Eugene, Oregon, USA). EEG was recorded continuously (1000 Hz sample rate; 0.1-400 Hz analogue bandpass) with Electrical Geodesics Inc. amplifiers (300-MΩ input impedance). Electrode impedances were kept below 40 kΩ, an acceptable level for this system (Ferree, Luu, Russell, & Tucker, 2001). Impedance checks were conducted between blocks, to ensure that impedance did not exceed this threshold. Data was

acquired using a common reference electrode (Cz), then later re-referenced offline to an average reference.

EEG Preprocessing

EEG data were processed twice, firstly in a way which was optimized for the performance of independent component analysis (ICA), and secondly in a way which was optimized for the production of ERP components. ICA weights from the first set of data could then be copied across in order to perform artefact correction in the ERP data. All EEG data were analyzed in Matlab (The MathWorks, Inc., Natick, Ma, USA), using the EEGLAB Toolbox (Delorme & Makeig, 2004), Wavelet Toolbox 4 (Misiti, Misiti, Oppenheim, & Poggi, 2007), and Spline Toolbox 3 (De Boor, 2005; Unser, Aldroubi, & Eden, 1992).

Preprocessing for ICA decomposition, the EEG data was downsampled to 250Hz for computational expediency, and the data was then bandpass filtered from 1 to 30Hz using a Butterworth filter implemented in ERPLAB (Lopez-Calderon & Luck, 2014). Next, channel locations were added, and channels that were flat for more than 5 seconds or were poorly correlated with adjacent channels (correlation threshold: 0.8) were removed and interpolated using a spherical-spline method (Perrin, Bertrand, & Pernier, 1987). The data was then re-referenced from Cz to an average reference in order to minimize the impact of reference site activity (Tucker, Liotti, Potts, Russell, & Posner, 1994). The data was then decomposed using an adaptive mixture independent component analysis (AMICA) (Palmer, J. A., Kreutz-Delgado, & Makeig, 2012) with the 'PCA keep option' to reduce the data rank to account for the number of interpolated channels. ICA weights were then stored in order to be applied to data which had been pre-processed for the production of ERPs.

For the production of ERPs, the EEG data was downsampled to 250Hz, and the data was then bandpass filtered from 0.1 to 30Hz using a Butterworth filter implemented in ERPLAB (Lopez-Calderon & Luck, 2014). Next, channel locations were added, and channels that were flat for more than 5 seconds or were poorly correlated with adjacent channels (correlation threshold: 0.8) were removed and interpolated using a spherical-spline method (Perrin et al., 1987). The data was then re-referenced from Cz to an average reference. The data were then segmented into epochs around the onset of the stimulus, with a prestimulus period of 100ms and a post-stimulus period of 1024ms. ICA weights were then copied over to this set of data in order to perform artefact correction. Subsequently, artifactual components were identified and removed using the Multiple Artifact Rejection Algorithm (Winkler, Haufe, & Tangermann, 2011) in conjunction with visual inspection. Lastly, epochs which contained any activity above 100 microvolts or below -100 microvolts were removed from the data. No participants had their data removed due to insufficient data quality.

Wavelet transform of ERP data

The wavelet transform decomposes the EEG signal $x(t)$, into a family of functions $\psi_{a,b}\,(t)$ which are obtained by dilating and shifting a mother wavelet $\psi(t)$ across the EEG signal. The scale parameter a stretches the wavelet function and adjusts its frequency content, while the position parameter b shifts the wavelet in the time domain.

$$\psi_{a,b}\,(t) = \left|a\right|^{-1/2} \psi\left(\frac{t-b}{a}\right) \quad a, b \in R, a \neq 0, \qquad [1]$$

The continuous wavelet transform (CWT_x) of a signal $x(t)$ at scale a and position b is defined by:

$$CWT_x(b,a) = \left\langle \mathbf{x}(t), |a|^{-t/2} \psi^*\left(\frac{t-b}{a}\right) \right\rangle$$

$$= |a|^{-1/2} \int_{\infty}^{\infty} x(t)\, \psi^*\left(\frac{t-b}{a}\right) dt, \qquad [2]$$

where * represents the complex conjugation and $\langle x, \psi \rangle$ represents the inner product. Equation [2] represents the multiresolution decomposition of the EEG signal into a set of frequency channels, which in the case $a = 2^j$ $(j = integer)$ would have one and the same bandwidth in a logarithmic scale. This property is known as constant relative bandwidth frequency analysis by octave band filters (Samar, Swartz, & Raghuveer, 1995), which allows for the examination of higher frequencies using shorter time windows and examining lower frequencies using longer time windows, thereby, maintaining the balance between spectral and temporal precision.

Wavelet coefficients are obtained by linearly shifting the wavelet across the EEG signal, and quantifying the degree of similarity between the wavelet and the EEG signal at each time point by taking the inner product of the signal and wavelet function, in order to estimate the amount of energy from a given frequency at each time point, and repeating this process for each frequency channel (Ademoglu et al., 1998; Samar et al., 1995; Samar, Bopardikar, Rao, & Swartz, 1999).

In the current study we used the quadratic B-spline wavelet function, because the quadratic B-spline wavelets have a wave shape similar to that of the frequency

components obtained by applying digital filtering to evoked EEG activity, and prior research suggests that the extraction of a component within the EEG signal is better when the wavelet shape closely mirrors the shape of the component itself (Basar, 1980; Samar et al., 1999). Additionally, the B-spline wavelets have near optimal time-frequency localization and even though they are not fully orthogonal, it does help to improve the distinctiveness of the ERP time-frequency transform (Unser et al., 1992).

A fast WT algorithm using a standard pyramidal filter scheme was utilized to decompose subjects' individual averaged ERPs (Ademoglu et al., 1998; Demiralp & Ademoglu, 2001; Yordanova et al., 2000). The application of a five-octave wavelet transform to the data yielded five sets of coefficients in the 64-128 Hz (high gamma), 32-64 Hz (gamma), 16-32 Hz (beta), 8-16 Hz (alpha), 4-8 Hz (theta), and 0.1-4 Hz (delta) frequency bands. The interpolation of the coefficients by quadratic spline functions was also used to reconstruct the EEG signal and to represent the full-time course of each frequency band, with color variation used to illustrate the amplitudes of the coefficients at a specific frequency and time (see Figures 6 and 7).

However, due to prior research demonstrating that activity within the delta- and theta-bands can account for the majority of the variance in the P3a and P3b (Başar-Eroglu et al., 1992; Kolev et al., 1997; Yordanova et al., 2000), our analysis focused only delta and theta coefficients. The time window used for delta and theta was 128 ms. The precise time localization of each delta and theta coefficient was: coefficient 0 (-100 - +28 ms), coefficient 1 (28-156 ms), coefficient 2 (156-284 ms), coefficient 3 (284-412 ms), coefficient 4 (412-540 ms), coefficient 5 (540-668 ms), coefficient 6 (668-796 ms), coefficient 7 (796-924 ms). Each time-frequency region is designated by a letter representing the frequency band (i.e., D for delta, and T for theta) and the coefficient

number representing the time window (e.g., the theta component in the 412-540 ms latency range will be noted as T4) (see Figure 4).

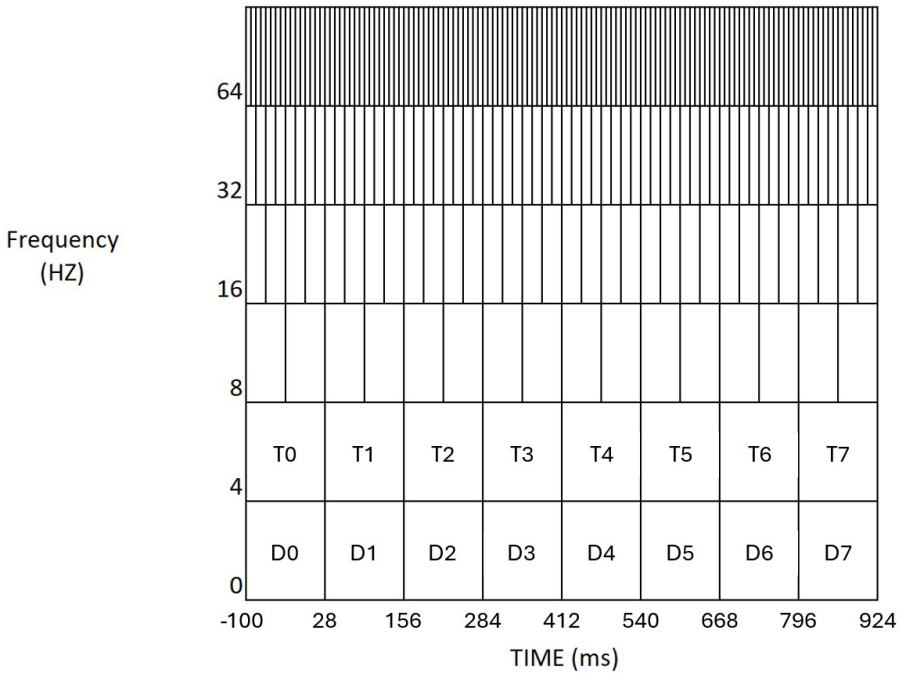

Figure 4. Schematic illustration of the time-frequency decomposition of the EEG data. The application of a five-octave wavelet transform to the data yields five sets of coefficients in the 64-128 Hz (high gamma), 32-64 Hz (gamma), 16-32 Hz (beta), 8-16 Hz (alpha), 4-8 Hz (theta) and 0.1-4 Hz (delta) frequency ranges, where each octave has the necessary number of coefficients for optimal temporal resolution.

Results

Behavioral Results

Independent sample t-tests revealed that there were no significant age-related changes to the hit rate t(48) <1, number of false alarms to distractors t(48) = -1.72, p = 0.92, or number of false alarms to standards t(48) <1. There was however a significant age-related change to reaction times t(48) = -2.59, p = 0.13 (see Table 1).

Table 1

3-Stimulus oddball task behavioural data

	Hit Rate (%)	False Alarm (Standards) (%)	False Alarm (Distractors) (%)	Reaction Time
Young	87.27 (7.61)	0.52 (0.65)	5.05 (13.98)	531 (77)
Old	85.79 (12.82)	4.47 (11.48)	2.5 (5.82)	602 (111)

Note. The standard deviations are presented in brackets

ERP Results

P3a (Distractor Oddballs). A 2 (age group: young, old) × 3 (electrode: Fz, Cz, Pz) mixed ANOVA was used to examine the age-related changes to the amplitude and topography of the P3a. The effect of age F(1,48) = 4.99, p = .03, and electrode F(1,48) = 157.17, p < .001, were both significant, as was the interaction between age × electrode F(1,48) = 104.37, p < .001. Follow-up analysis showed that there was a significant age-related increase to the P3a at electrode Fz (p <.001), and a significant age-related decrease to the P3a at electrodes Cz (p = .009) and Pz (p <.001) (see Figure 5).

Age-related changes to P3a latency was determined by averaging the peak latency across the 3 midline electrode sites (Fz, Cz, and Pz) for each individual and performing an independent sample t-test to determine if there was any age-related changes to the

efficiency of processing for distractors. The analysis revealed a significant age-related increase to the latency of the P3a $t(48) = -22.76$, $p < .001$.

P3b (Target Oddball). A 2 (age group: young, old) × 3 (electrode: Fz, Cz, Pz) mixed ANOVA was also used to examine the age-related changes to the amplitude and topography of the P3b. The effect of age $F(1,48) = 46.02$, $p < .001$, and electrode $F(1,48) = 156.12$, $p < .001$, were both significant, as was the interaction between age × electrode $F(1,48) = 80.42$, $p < .001$. Follow-up analysis showed that there was a significant age-related increase to the P3b at electrode Fz ($p < .001$), and Cz ($p < .001$), as well as a significant age-related decrease to the P3b at electrode Pz ($p = .009$) (see Figure 5).

Age-related changes to P3b latency was determined by averaging the peak latency across the 3 midline electrode sites (Fz, Cz, and Pz) for each individual and performing an independent sample t-test to determine if there was any age-related changes to the efficiency of target processing. The analysis revealed a significant age-related increase to the latency of the P3b $t(48) = -85.19$, $p < .001$.

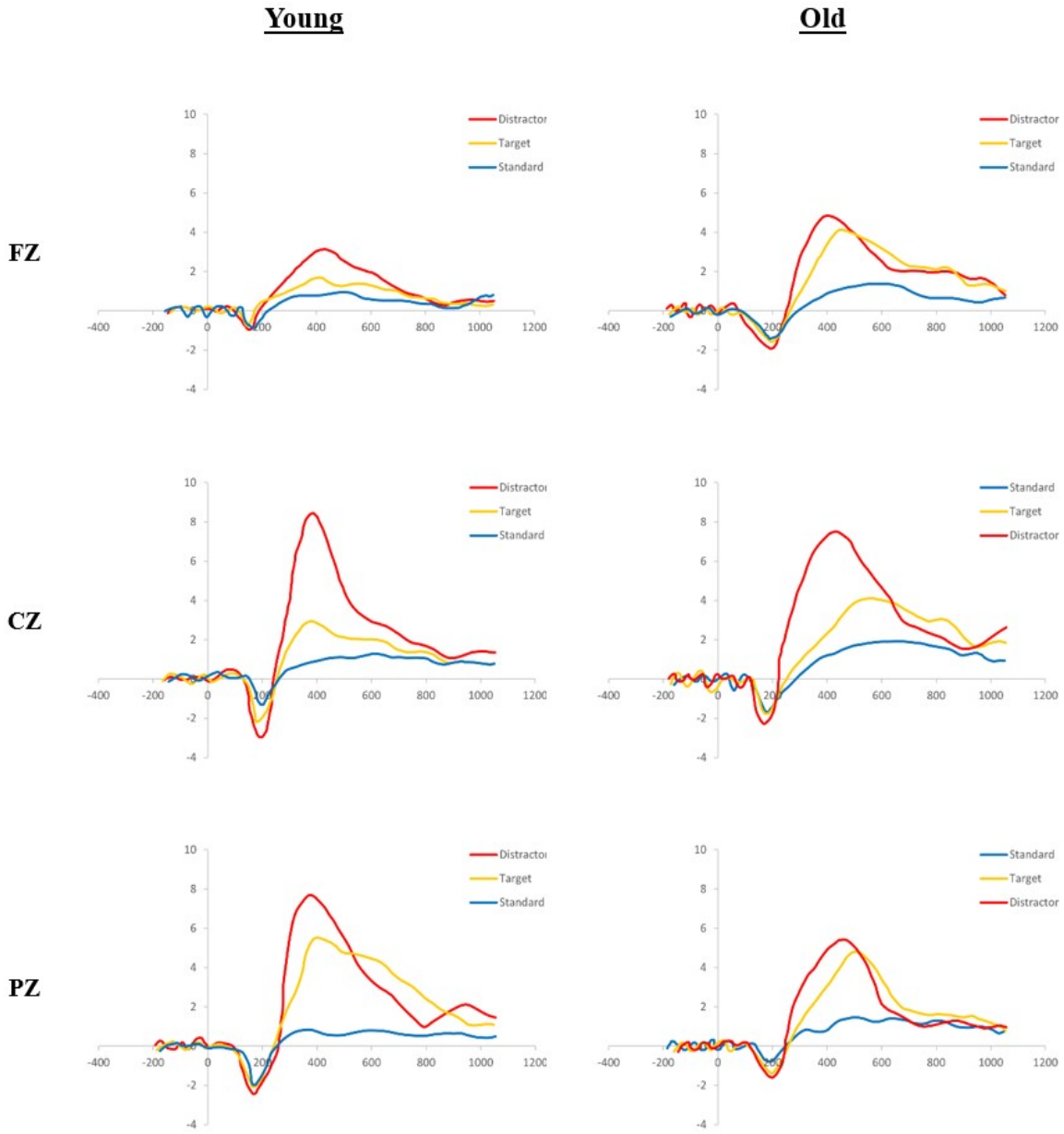

Figure 5. Grand average of target, distractor and standard ERPs at Fz, Cz and Pz for younger and older adults.

ERP Wavelet Analysis Results

Our analysis focused only on the frontocentral (FCz) theta-band activity during the T3 and T4 time window, and centroparietal (CPz) delta-band activity during the D4 and D5 time window. These coefficients were selected based on when theta-band and delta -band activity peaked in response to the presentation of the oddball stimuli.

Independent sample t-tests revealed no significant age-related changes to theta-band activity during the T3 window in response to either the presentation of targets $t(48) < 1$, or distractors $t(48) < 1$. There was however, a significant age-related increase to theta-band activity during the T4 window in response to both targets $t(48) = -10.22$, $p < .001$, as well as, distractors $t(48) = -22.15$, $p < .001$.

Analysis of the age-related changes to delta-band activity revealed a significant age-related increase to delta-band activity during both the D4 window $t(48) = -5.48$, $p < .001$, and the D5 window $t(48) = -2.82$, $p = 0.03$, in response to the presentation of distractors. In addition there was also a significant age-related decrease to delta-band activity during the D4 window $t(48) = 4.73$, $p < .001$, and the D5 window $t(48) = 3.19$, $p = .001$, in response to the presentation of targets.

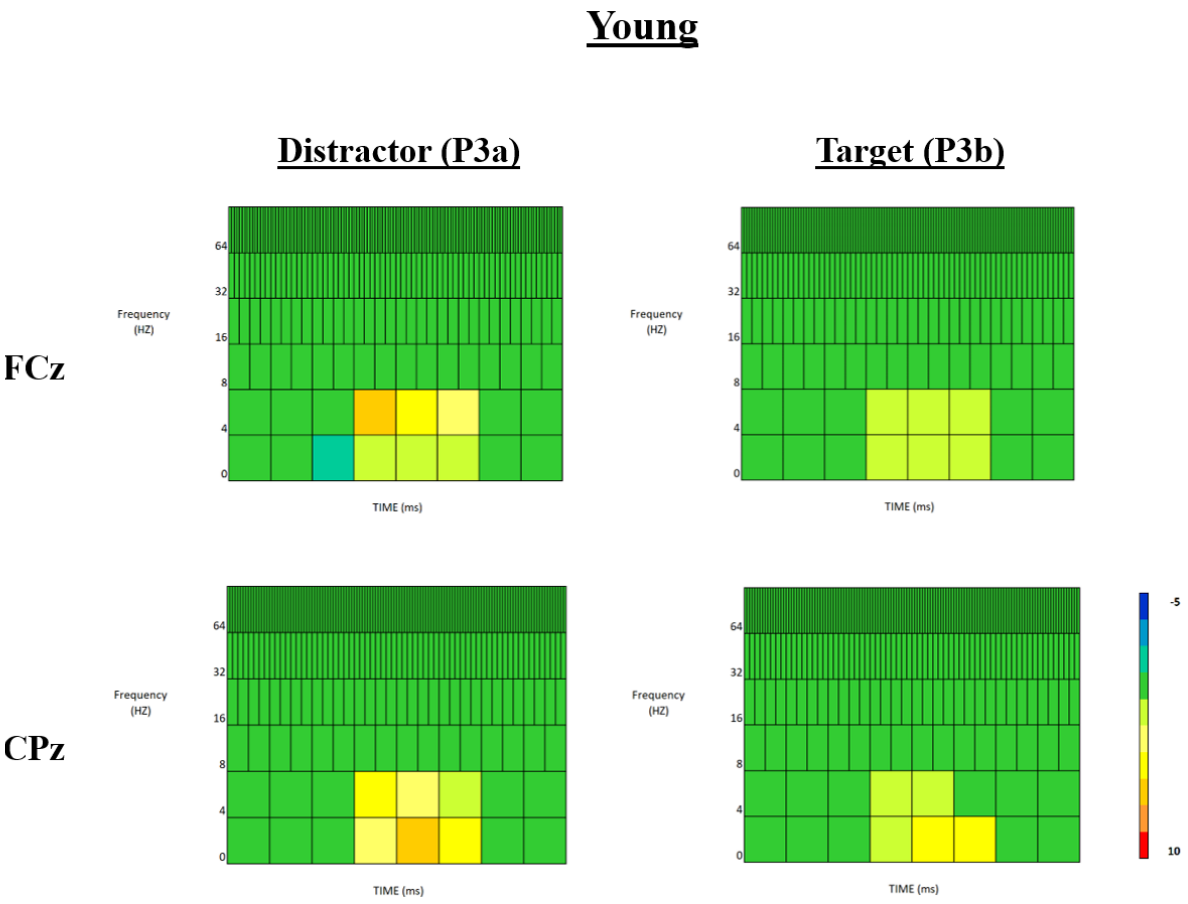

Figure 6. Time-frequency representation of non-target and target ERPs for younger adults. The amplitudes of the wavelet coefficients are encoded in colour.

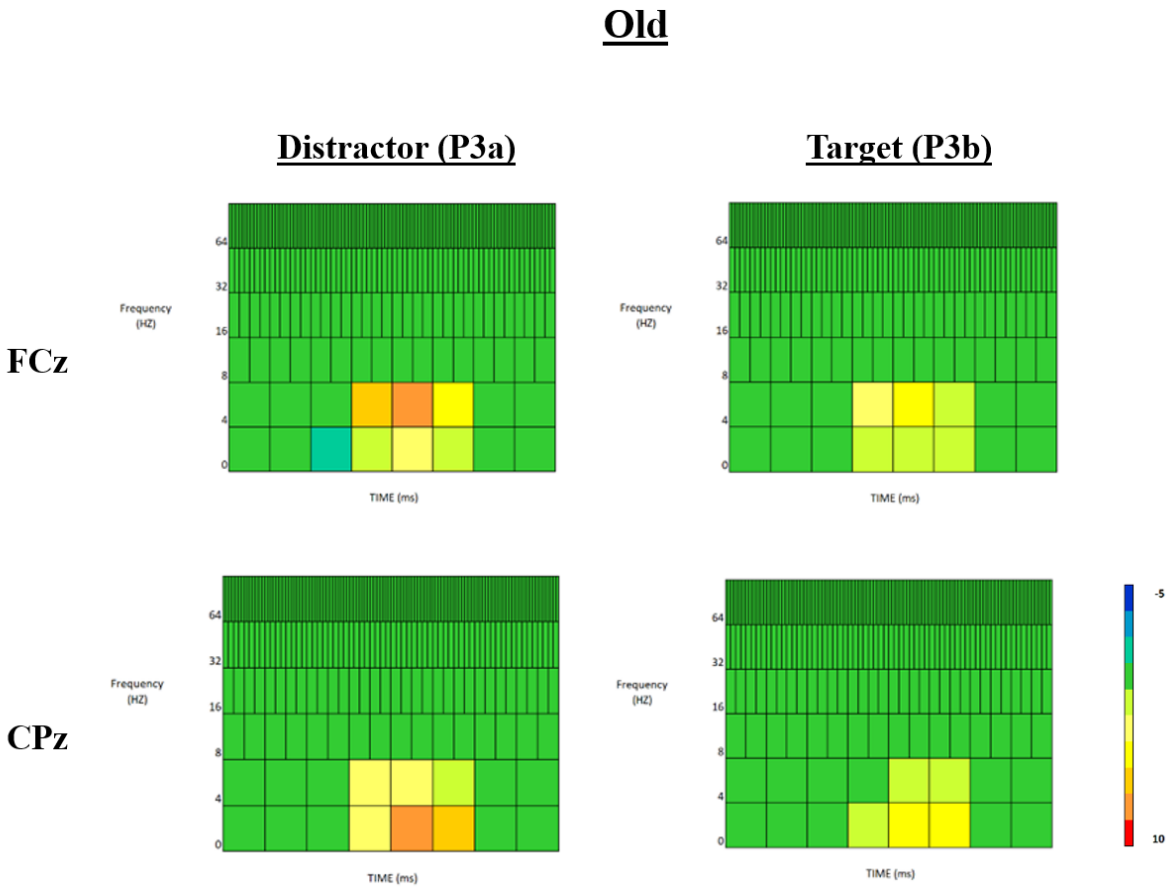

Figure 7. Time-frequency representation of non-target and target ERPs for older adults. The amplitudes of the wavelet coefficients are encoded in color.

Discussion

The goal of the first experimental chapter was to examine the age-related changes to the P3a and P3b, as well as to determine the extent to which these changes reflect changes to attentional orienting or stimulus evaluation/context updating processes. The analysis of the ERP data revealed several notable age-related changes to the P3a and P3b. This included 1) a significant age-related attenuation to both the P3a and P3b, 2) a significant age-related delay to the latency of both the P3a and P3b, as well as, 3) a significant 'anterior-shift' to the topography of both the P3a and P3b in older adults, caused by the increased amplitude of these components at frontal electrode sites, coupled with a reduction of the amplitude of these components at posterior electrode sites. The age-related reduction to the amplitude of the P3a and P3b is believed to reflect an overall decrease in the amount of neural resources available for the processing of unexpectedly presented stimuli; while the delay to the latency of the P3a and P3b is believed to reflect an age-related slowing of information processing that impacts how quickly unexpectedly presented stimuli are processed in older adults (Fein & Turetsky, 1989; Fjell & Walhovd, 2003; Fjell et al., 2007; Fjell et al., 2009; Polich, 1996; Walhovd et al., 2008). The age-related changes to the topography of the P3a and P3b has commonly been viewed as a reflection of the age-related changes to the way the brain processes unexpectedly presented stimuli, although the nature of these changes has been rather controversial (Alperin et al., 2014; Fjell & Walhovd, 2001; Fjell et al., 2005).

In the current study, a time-frequency decomposition of the ERP data was performed to explore exactly how the age-related changes to the attentional orienting and stimulus evaluation/context updating processes contribute towards the age-related changes to the topography of the P3a and P3b. The results of this analysis revealed a significant age-related increase to centroparietal delta-band activity in response to

distractors, and a significant age-related decrease to centroparietal delta-band activity in response to target stimuli. Given that a similar pattern of changes in delta-band activity is seen in younger adults when the target/standard discrimination is made more difficult by increasing the degree of perceptual similarity between the target and standard stimuli (Demiralp et al., 2001); the current results suggests that older adults may have more difficulty distinguishing between target and standard stimuli leading to the significant age-related decrease in delta-band activity in response to targets (Başar-Eroglu et al., 1992; Demiralp et al., 2001; Yordanova et al., 2000). The increased focus on target/standard discrimination also leads to a larger 'surprise-related' signal in response to distractors which are perceived as more distinctive in comparison (Polich, 2007). The increase in perceived distinctiveness results in a larger update to the mental model of the environment and this is reflected by the increase in delta-band activity in centroparietal regions (Başar-Eroglu et al., 1992; Demiralp et al., 2001; Yordanova et al., 2000).

Additionally, there was also evidence of a significant age-related increase to theta-band activity within the frontocentral areas in response to both targets and distractors. This suggests that older adults dedicate more attentional resources towards the processing of unexpected stimuli, and this occurs regardless of the task relevance of the stimuli. However, because the deployment of additional attentional resources only occurs during the T4 window, it also suggests that the deployment of attentional resources may occur more slowly in older adults (Salthouse, 2000). Additionally, although the increased processing of distractors is commonly interpreted as a negative consequence of the ageing process; several studies have shown that the increase allocation of attentional resources towards any potentially behaviourally relevant stimuli may actually be an adaptive mechanism that helps to compensate for age-related neurophysiological and sensory declines (Daffner et al., 2005; Healey et al., 2008; Riis et al., 2008; Rowe, Valderrama,

Hasher, & Lenartowicz, 2006). For example, a study by Riis et al. (2008) showed that cognitively higher performing older adults dedicated more attentional resources towards the processing of both target and distractors compared to younger adults or their more cognitively average counterparts. It is suggested that older adults with a higher level of cognitive reserve may compensate for age-related declines in information processing speed by appropriating more resources towards the processing of potentially behaviourally relevant stimuli (Daffner et al., 2005; Healey et al., 2008; Riis et al., 2008). In contrast, younger adults do not need to engage additional frontal resource for the processing of unexpected stimuli and can relegate processing towards posterior cortical regions, whilst lower performing older adults are unable to effectively engage the additional frontal resources necessary to perform the task successfully (Daffner et al., 2005; Riis et al., 2008).

Overall, the pattern of age-related changes to frontocentral theta-band activity and centroparietal delta-band activity in the current study suggests that older adults may suffer from age-related perceptual changes which impacts their ability to perform the target/standard discrimination and older adults may attempt to compensate for these changes by appropriating more resources towards the processing of unexpected stimuli, and this processes is reflected in the time-domain as an 'anterior-shift' to the P3a and P3b. This interpretation of the data is consistent with the results from an EEG/fMRI fusion study conducted by O'Connell et al. (2012) which showed that the age-related 'anterior-shift' to the topography of both the P3a and P3b is caused by an increased recruitment of frontal areas including the dorsolateral prefrontal cortex and inferior frontal cortex coupled with a decrease in the activity within the inferior parietal cortex. Unfortunately, despite the significant strides that have been made towards understanding how localized neural changes affect the topography of the P3a and P3b in recent years,

little is known about how the interaction between these regions changes as we age, and how these changes affect the topography of these components (Fjell et al., 2005; O'Connell et al., 2012). Examining the age-related changes to the functional and/or effective connectivity between the frontoparietal regions involved into the generation of the P3a and P3b will help provide further insights into the functional significance of the age-related changes to the topography of these components (Friston, Karl J., 2011).

Chapter 3: Age-related Changes to the P3a and P3b—A Dynamic Causal Modelling Study

In addition to the age-related changes to amplitude and latency of the P3a and P3b, numerous studies have also noted a significant 'anterior-shift' to the topography of both the P3a and P3b components (Fabiani et al., 1998; Fjell et al., 2005; Friedman et al., 1997; O'Connell et al., 2012). There is however considerable debate about whether this shift represents older adults' increased reliance on frontally-mediated control mechanisms to support task performance (Alperin et al., 2014; Daffner et al., 2006; Riis et al., 2008), or if it simply represents a maladaptive response to frontal lobe deterioration that results in a failure to habituate to the novelty of the oddball stimuli (Fabiani et al., 1998; West et al., 2010). In the current chapter, we explore both possibilities by using dynamic causal modelling (DCM) to uncover the neural dynamics responsible for the 'anterior-shift' of the P3a and P3b in older adults. The analysis focused on the age-related changes to the interaction between several key regions involved in the generation of the P3a and P3b, including the visual sensory regions, the IPS, the DLPFC and the ACC.

Methodology

Participants and Data Collection

The participants and data used in the current chapter are the same as those used in chapter 2, with the exception of the removal of the data of one younger and one older participant due to unique skull morphology. This left a final sample of 24 younger adults (M= 24.08, SD= 3.88) and 24 older adults (M= 73.63, SD= 5.29). Please see chapter 2 methodology section for data collection and pre-processing details. The pre-processed data was then imported into SPM 12 (https://www.fil.ion.ucl.ac.uk/spm/).

Dynamic Causal Modelling

DCM was used to examine the age-related changes to the network dynamics responsible for the generation of the P3a and P3b. Each DCM consisted of a network of interacting cortical sources that were assembled according to the connectivity rules described by (Felleman & Van Essen, 1991). The activity of each source was modelled by the hierarchical neural mass model referred to as the ERP model (see Figure 8) (David et al., 2006; Kiebel, David, & Friston, 2006). This model involves a tri-partitioning of the cortical sheet into supra-granular, granular, and infra-granular layers. The activity of each source is represented by the activity of three neural subpopulations assigned to each one of these cortical layers. A population of excitatory spiny stellate cells in the granular layer, inhibitory interneurons in the supra-granular layer, and deep pyramidal cells assigned to the infra-granular layer. All extrinsic cortico-cortico connections are mediated by the axons of excitatory pyramidal cells, which receive a combination of excitatory and inhibitory inputs from local interneurons through intrinsic connections. Inputs to the model are fed into the granular layer and have the same characteristics as bottom-up or forward connections, which originate in the infra-granular layers and terminate in the granular layer. The top-down or backward connections link agranular layers. While, lateral connections originate in the infra-granular layer and target all layers. Within each subpopulation, the progression of neuronal states rests upon two operators. The first operator is a convolution kernel that transforms the pre-synaptic inputs into an average postsynaptic membrane potential, which determines the maximum amplitude of the post synaptic potential, and the rate of passive delays (i.e., a rate constant) (David & Friston, 2003). The second operator is a sigmoidal function, which transforms the average postsynaptic membrane potential into an average firing rate, which serves as the input into other subpopulations (David & Friston, 2003).

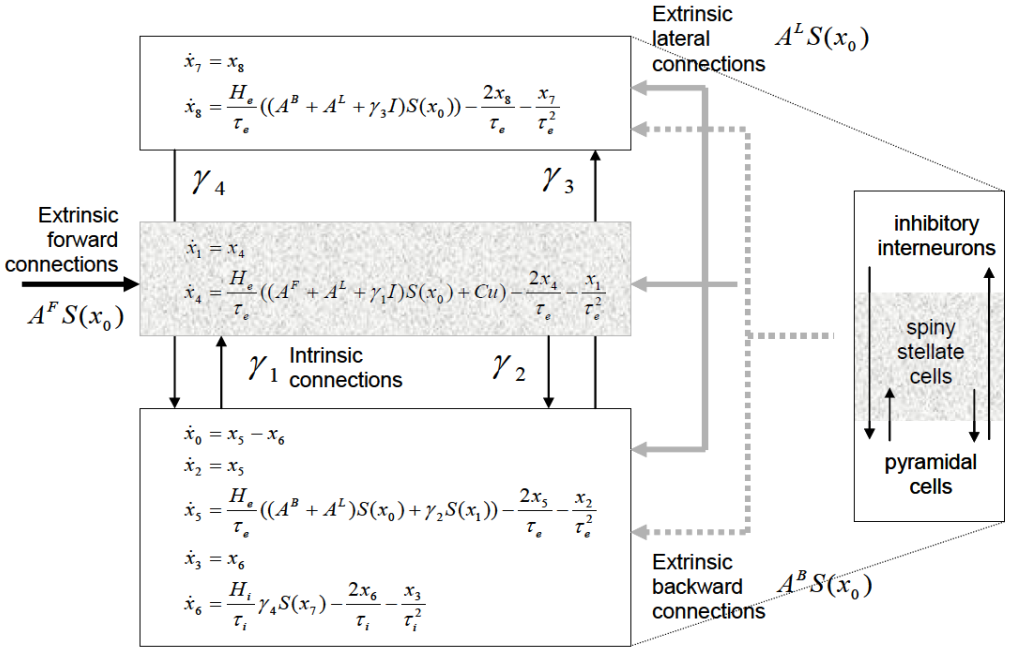

Figure 8. A diagrammatic representation of the hierarchical neural mass model used to model electrophysiological responses. The state equations embody the connection rules described by Fellerman and Van Essen (1991), and reflect the dynamics of the source regions. The diagram is adapted from "Dynamic causal modelling of evoked responses in EEG and MEG", by David et al. (2006), NeuroImage, 30, 1255-1272.

Once the neuronal model was specified in terms of which regions receive inputs, how the regions are connected, and which coupling parameters are modulated by experimental factors, it was passed through an electromagnetic forward model which depicts how source activity is reflected at the scalp level (Kiebel et al., 2006). Each source was represented as an equivalent current dipole (ECD), with lead field mapping parameterised via the location and orientation of each dipole (Kiebel et al., 2006). The location parameters are provided by the Montreal Neurological Institute (MNI) coordinates and the orientation parameters had a prior mean of zero, and a variance of 256mm^2.

The DCM was then inverted using a variational bayes optimization scheme. This involves iteratively updating the posterior moments (mean and covariance of coupling

parameters) until the point of convergence (i.e., the point that provides the best fit between the observed and the predicted response under complexity constraints). The inversion procedure provides the posterior probability of model parameters, which is used to make inferences about how coupling parameters are modulated by experimental factors, and the free energy approximation to the log-model evidence which can be utilized for model comparison purposes (Friston, Karl J., Harrison, & Penny, 2003).

Individual DCM Specification

Given the considerable evidence which suggests that the generation of the P3a and P3b share the same underlying neural architecture, we used the same generative model for both the P3a and P3b (Bledowski et al., 2004; Linden et al., 1999; Linden, 2005). Each participant's DCM consisted of the dorsal anterior cingulate cortex (dACC) (MNI coordinates [0, 20, 30]), bilateral MOG (MNI coordinates [±36, -78, 2]), IPS (MNI coordinates [±32, -57, 43]), and DLPFC (MNI coordinates [±30, 43, 23]). The regions were connected as shown in Figure 9. Each DCM modelled a 0-600 ms time window, and thalamic input entered into MOG bilaterally with an 80 ms delay, and 16ms variation. The models provided a good fit to the data. For the distractor condition, the models explained an average of 87.58% of the variance in young adults' data and 78.83% of variance in older adults' data. For the target condition, the models explained 79.12% of the variance in younger adults' data and 77.44% in older adults' data.

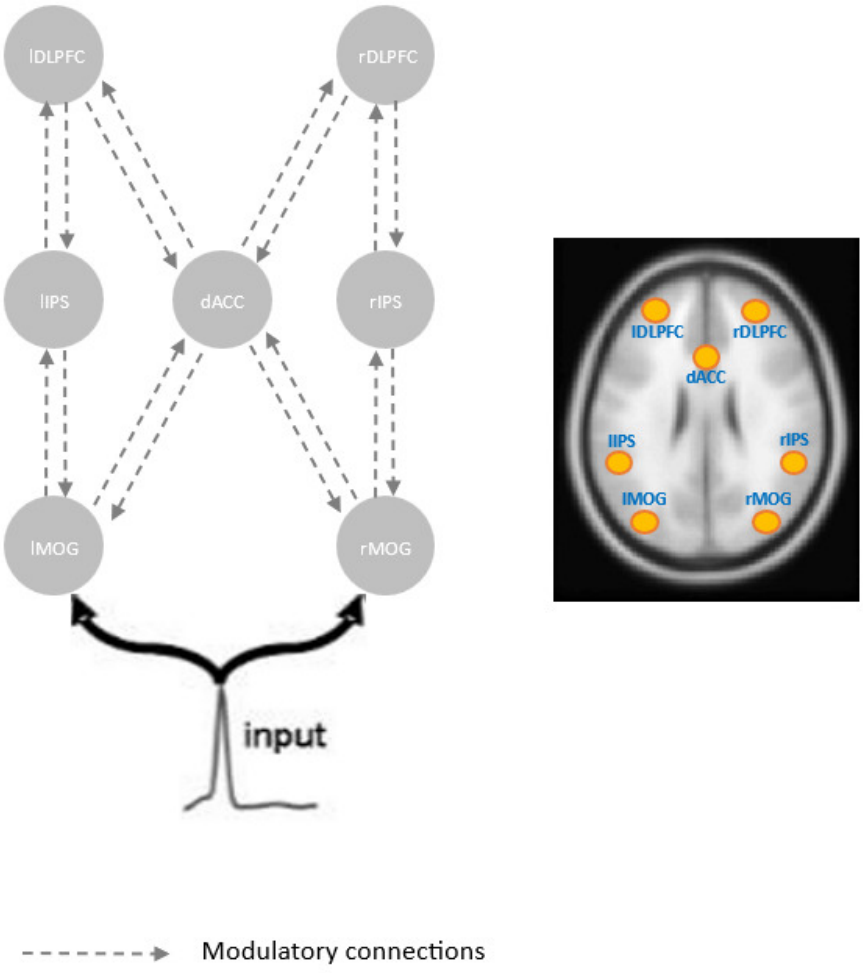

Figure 9. Model specification for both P3a and P3b (left). The regions are connected with both feedforward and feedback connections, with broken lines representing the regions that were allowed to be modulated by experimental perturbation. Sources of activity were modelled as dipoles (estimated posterior moments and locations), and are superimposed in an MRI of a standard brain in MNI space (right).

Parametric Empirical Bayes and Bayesian Model Reduction

PEB was used to examine the impact of aging on the modulation of connectivity strengths (Friston et al., 2016, 2015). PEB is a hierarchical modelling scheme in which second level (between-subject) empirical priors are used to constrain subject specific (first-level) parameter estimates (Friston et al., 2016). This makes PEB a particularly useful technique when participants can be assumed to share the same underlying neural architecture and differ only in their connection strengths and the extent to which these connection strengths are modulated by experimental factors (Friston, Karl, Zeidman, & Litvak, 2015; Friston, Karl J. et al., 2016). By allowing priors from the group level to constrain subject-specific parameters we are also able to obtain more robust parameter estimates which reduces the impact that outliers have on the results and this also helps to mitigate the difficulties in source localization that arise from the age-related increases in neural noise (Friston, Karl et al., 2015; Friston, Karl J. et al., 2016; Zeidman et al., 2019).

PEB uses a second level GLM that enables the estimation of every combination of between-subject effect and every first level parameter (i.e., within-subject DCM connections) (Pinotsis et al., 2016; Zhou et al., 2018). In the current study, the design matrix consisted of two columns representing 1) an overall group effect, and 2) the effect of age. To search over nested PEB models, Bayesian model reduction (BMR) was then applied to each subject's inverted DCM to prune away parameters that did not contribute towards the model evidence. Only the posterior estimates of parameters that exhibited a posterior probability (Pp) >0.95 are reported.

Results

DCM Results: P3a (Distractor Oddball)

For both younger and older adults, the generation of the P3a involved the modulation of both feedforward and feedback connections between the MOG, IPS, and DLPFC bilaterally. There was also evidence of significant modulation of feedforward connections from the left and right MOG to the dACC , and from the dACC to the left and right DLPFC. Additionally, compared to younger adults, older adults showed a significant increase in the modulation of feedforward connectivity between the dACC and left DLPFC (please see *Figure 10*).

DCM Results: P3b (Target Oddball)

For both younger and older adults, the generation of the P3b involved the modulation of feedforward connections from the left and right MOG to the dACC. There was also evidence of a significant modulation of feedforward connections from the right MOG to the right IPS, and from the right IPS to the right DLPFC. Additionally, compared to younger adults, older adults showed weaker modulation of feedforward connections from the left and right MOG to the dACC , and from the dACC to both the left and the right DLPFC. Lastly, there was also evidence of a significant age-related increase in the modulation of feedback connections from the right DLPFC to the right IPS, and from the right IPS to the right MOG (please see *Figure 10*).

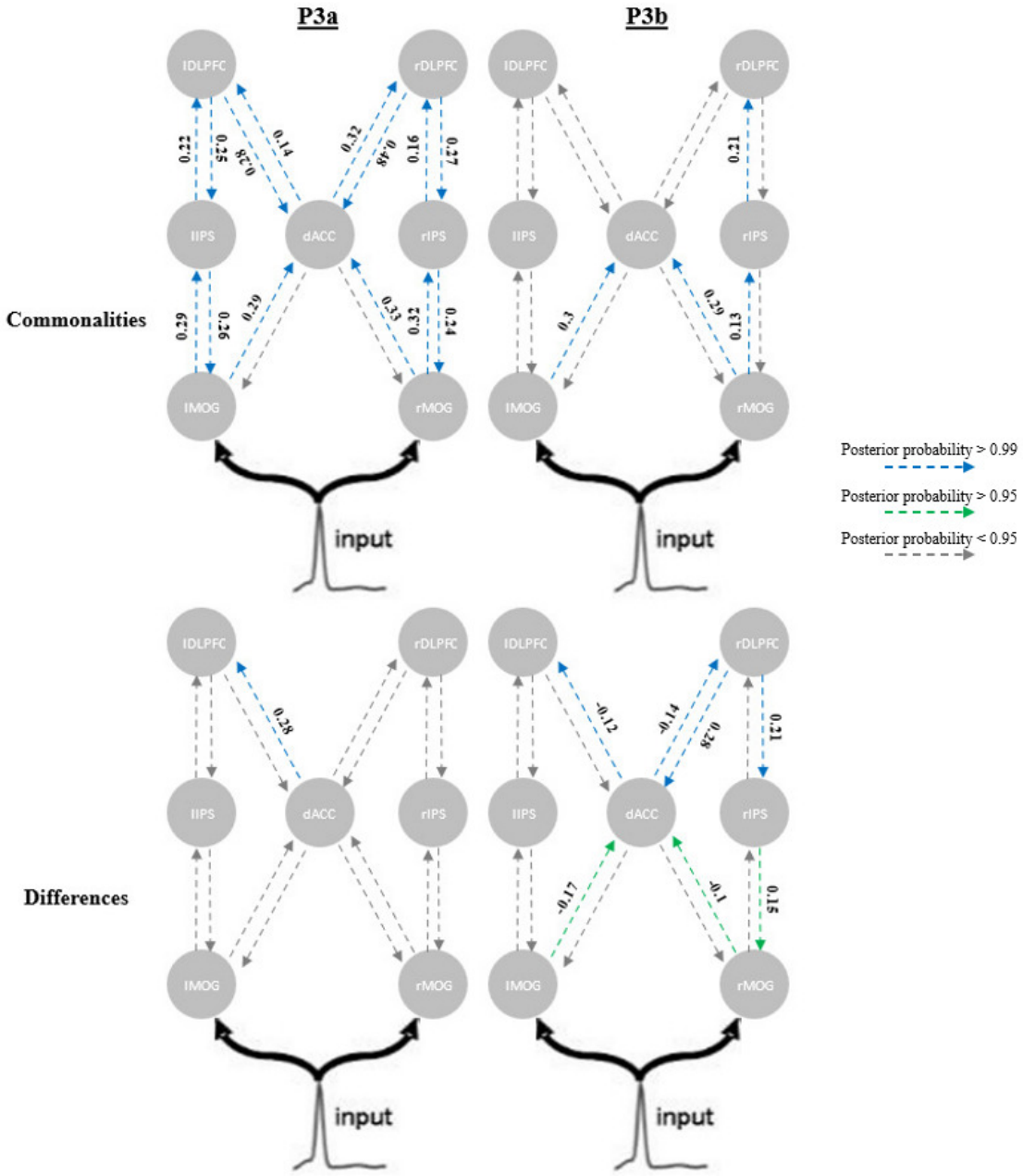

Figure 10. The DCM results showing the connections that were significantly modulated by the presentation of distractors (left panel) and the presentation of targets (right panel). The commonalities between younger and older adults are presented in the top panel, while the differences between younger and older adults are represented in the bottom panel. In the top panel, positive posterior parameter estimates indicate an increase in connectivity strength, while negative posterior parameter estimates represent a decrease in connectivity strength between regions. In the bottom panel, positive posterior parameter estimates indicate stronger modulation of connectivity in older adults, while negative posterior parameter estimates indicate weaker modulation of connectivity in older adults relative to younger adults.

Discussion

The goal of the second experimental chapter was to determine the functional significance of the 'anterior-shift' of the P3a and P3b in older adults by exploring the underlying mechanisms responsible for this shift. This involved examining the network dynamics responsible for the generation of the P3a and P3b in a group of younger and older adults, and identifying the commonalities and differences between the two groups. The results indicated a considerable degree of overlap in the network dynamics responsible for the generation of the P3a in both younger and older adults. For both younger and older adults, the generation of the P3a involved significant modulation of both feedforward and feedback connections between the MOG, IPS, and DLPFC bilaterally. Additionally, there was a significant increase in the strength of feedforward connections between the MOG, dACC and DLPFC. However, there was no evidence that oddball processing modulated the strength of feedback connections between the dACC and MOG in either younger or older adults. This suggests that the dACC may only be indirectly involved in the attentional modulation of sensory processing (Botvinick, Matthew, Nystrom, Fissell, Carter, & Cohen, 1999; Botvinick, Matthew M., Cohen, & Carter, 2004), while the DAN regions are more directly involved in the disengagement of attentional resources from the repeatedly presented standard stimuli, and the subsequent reallocation of attentional resources towards the oddball stimulus (Bledowski et al., 2004; Bocquillon et al., 2011). On the other hand, there was little overlap in the network dynamics responsible for the generation of the P3b. Both younger and older adults showed a significant modulation of the feedforward connections from the left and right MOG to the dACC, they also showed an increase in feedforward connections from the right MOG to the right IPS, and from the right IPS to the right DLPFC. The limited overlap in the network dynamics responsible for the generation of the P3b in younger and

older adults may be due to the high degree of perceptual similarity between targets and standards used in the current study. This may have made it harder for older adults to easily distinguish targets from the repeatedly presented standard stimuli, which is consistent with the age-related changes to the network dynamics responsible for the generation of the P3b discussed in the next paragraph, and is also supported by the fact that older adults did appear to have a marginally increased number of false alarms to standards; although it must be noted that this effect did fail to reach statistical significance.

Overall, the current results suggest that although there is a significant 'anterior-shift' to both the P3a and P3b, the mechanisms underlying this shift are not the same for both components. For the P3a, older adults showed a significantly greater increase in the connectivity between the dACC and the left DLPFC compared to younger adults. Since the strength of feedforward connections between the dACC and the DLPFC corresponds to the degree of expectancy violation (Botvinick, Matthew M. et al., 2004; Carter & Van Veen, 2007; Wang et al., 2005), the current results suggest that the 'anterior-shift' of the P3a may stem from older adults' failure to habituate to the repeated presentation of the distractor stimuli, which leads to a larger orienting response towards these stimuli when they are presented (Fabiani et al., 1998; West et al., 2010). In contrast, there were more pronounced age-related changes to the network dynamics responsible for the generation of the P3b. This involved an age-related decrease in the modulation of feedforward connections from the left and right MOG to the dACC, and weaker modulation of feedforward connections between the dACC to the left and right DLPFC. Additionally, older adults also exhibited significant modulation of feedback connections from the right DLPFC to the right IPS, and from the right IPS to the right MOG which was not present in younger adults. The decrease in feedforward connections suggests that older adults

may have had more difficulty distinguishing targets from standards. Although it is unclear if this difficulty stems from perceptual declines or declines in posterior cortical regions. Together, the weaker modulation of feedforward connections and the increase in strength of feedback connections in older adults suggests that the 'anterior-shift' of the P3b reflects the compensatory activation of prefrontal regions to compensate for the reduced activity in posterior cortical regions caused by age-related sensory declines (O'Connell et al., 2012). The lateralisation of the age-related changes to the network dynamics responsible for the generation of the P3a and P3b also maps onto a general trend in the functional imaging literature which suggests that the left hemisphere is more involved in distractor processing, whilst the right hemisphere is more involved in target processing (Bledowski et al., 2004; Eichele et al., 2005; Kirino, Belger, Goldman-Rakic, & McCarthy, 2000; Solbakk et al., 2008).

One important thing to note is that because our ability to accurately estimate the modulation of coupling strengths rests upon our ability to accurately characterise the temporal dynamics of the system, the issues with the current integration scheme used may have led us to inadvertently underestimate the age-related changes to the network dynamics responsible for the generation of the P3a and P3b (Lemaréchal, George, & David, 2018; Schöbi et al., 2021). Simply put, the parameters that describe the temporal flow of information across the system (e.g., conduction delays) need to be estimated precisely during the model inversion process, and the ability to precisely estimate these parameters depends on the method used to integrate the delay differential equations that characterise the propagation of information across the system (Lemaréchal et al., 2018; Schöbi et al., 2021). Unfortunately, the standard implementation of DCM for electrophysiological data (SPM12), uses an integration scheme that assumes that the system is locally linear (in time) (David et al., 2006; Lemaréchal et al., 2018; Schöbi et

al., 2021). However, given that signal conduction velocity is determined by a combination of highly nonlinear processes such as the density of afferent axonal connection, the concentration of neurotransmitters in the synaptic cleft, and the availability of receptors at the postsynaptic site, the current integration scheme leads to a systematic underestimation of parameter estimates (Shettigar, Yang, Tu, & Suh, 2022). Furthermore, because the degree of inaccuracy is accentuated at longer or more variable delays, the age-related changes to the microstructural integrity of white matter pathways (Bennett & Madden, 2014; Madden, Bennett, & Song, 2009), and reduction in the number of neurotransmitter postsynaptic receptor sites (Bäckman et al., 2010; Kaasinen et al., 2000; Volkow et al., 2000) may have led to an underestimation of the age-related changes to the network dynamics responsible for the generation of the P3a and P3b.

Lastly, although the results from the current study provides some valuable insights into how the network dynamics involved in the generation of the P3a and P3b change as we age, it does not enable us to determine if these changes are the result of a decline to the health and fitness of the frontoparietal network regions responsible for the generation of the P3a and P3b, or whether it simply reflects a shift in approach to the task. Therefore, in the next chapter we focused on examining the age-related changes to the intrinsic functional connectivity between the frontoparietal regions responsible for the generation of the P3a and P3b.

Chapter 4: Relationships between Intrinsic Functional Connectivity and the Age-related Changes to the P3a and P3b

Intrinsic functional connectivity refers to the inherent connectivity between regions that is not due to external sensory stimulation or external task demands (Andrews-Hanna et al., 2007; Fox et al., 2005; Fox & Raichle, 2007; Raichle, 2010). Therefore, examining the age-related changes to the level of intrinsic connectivity of a network provides a reliable approximation of the age-related changes to the integrity of the network (Betzel et al., 2014; Damoiseaux, 2017) In the current chapter, we utilized a graph theoretical approach to examine the age-related changes to the intrinsic connectivity between the frontoparietal network regions responsible for the generation of the P3a and P3b.

Graph theory-based approaches model the brain as a complex network represented graphically by a collection of nodes and edges (Bassett & Sporns, 2017; Sporns & Honey, 2006). Nodes can represent distinct brain areas, EEG electrodes or MEG channels, while the connections between the nodes are referred to as edges. Nodes that are directly connected through one edge are referred to as neighbours. On the other hand, a series of edges connecting distant nodes are referred to as a path. Once the network has been constructed, the complex network measures that characterize the network organizational structure can be extracted. In the current study, we focused on the age-related changes to global and local efficiency (see methodology section for details about calculation of these metrics). Global efficiency represents the degree of functional integration within a network, while local efficiency represents the degree of functional segregation within a network (Rubinov & Sporns, 2010). Typically, functional brain networks balance the need for functional integration and functional segregation by exhibiting both high global efficiency and high local efficiency (Latora & Marchiori,

2001; Tononi, Sporns, & Edelman, 1994). This balance allows networks to maximize the efficiency of information transfer while minimizing the high metabolic costs associated with long polysynaptic pathways (Bassett & Sporns, 2017; Latora & Marchiori, 2001; Rubinov & Sporns, 2010; Sporns & Honey, 2006; Watts & Strogatz, 1998). Unfortunately, age-related changes to the global and/or local efficiency of the frontoparietal network may impact the network's ability to function effectively (Deery, Di Paolo, Moran, Egan, & Jamadar, 2021). Therefore, in the current chapter we examined the age-related changes to the efficiency of the frontoparietal network and explored the relationship between network efficiency and the amplitude and latency of the P3a and P3b components.

Methodology

Participants

See chapter 2 methodology for participant details.

EEG Resting-State Task

Participants participated in a 7-minute eyes-opened resting-state task prior to performing the 3-stimulus oddball task described in chapter 2's methodology section. Participants were asked to relax and to keep their eyes fixated on the large fixation cross centred in the middle of the screen, and to focus on the sound of their breathing. Participants were instructed to focus on external stimuli while in a relaxed state in order to minimize the possibility of mind wandering. Participants were also told to refrain from excessive movements and to try to keep eye movements to a minimum. At the end of the resting state phase, participants were asked about whether or not they had any internal thoughts during the task. The 2 older adults that reported thinking and/or singing during the resting-state task, repeated the resting-state task again after a brief rest period.

EEG Recording.

The electroencephalography (EEG) recordings were conducted in an electrically shielded room (IAC Noise Lock Acoustic - Model 1375, Hampshire, United Kingdom) using 128-channel Ag/AgCl electrode nets (Tucker, 1993) from Electrical Geodesics Inc., (Eugene, Oregon, USA). EEG was recorded continuously (1000 Hz sample rate; 0.1-400 Hz analogue bandpass) with Electrical Geodesics Inc. amplifiers (300-MΩ input impedance). Electrode impedances were kept below 40 kΩ, an acceptable level for this system (Ferree et al., 2001; Luu & Ferree, 2005). Impedance checks were conducted between blocks, to ensure that impedance did not exceed this threshold. Data was acquired using a common reference electrode (Cz), then later re-referenced offline to an average reference.

Resting-State Data Pre-Processing & Network Analysis.

Prior to the construction of the adjacency (connectivity) matrix, the resting-state EEG Data was preprocessed using the EEGLAB toolbox extension (Delorme & Makeig, 2004) in order to remove any ocular and movement artifacts. First, the EEG data was downsampled to 500Hz and then bandpass filtered from 1 to 30Hz using a Butterworth filter implemented in ERPLAB (Lopez-Calderon & Luck, 2014). Next, channel locations were added, and channels that were flat for more than 5 seconds or were poorly correlated with adjacent channels (correlation threshold: 0.8) were removed and interpolated using a spherical-spline method (Perrin et al., 1987). A 2-step artefact correction procedure was used. In the first step, artefact subspace reconstruction (ASR) was used to mitigate the impact of occasional large-amplitude artifacts, and provide a better ICA decomposition (Chang, Hsu, Pion-Tonachini, & Jung, 2018; Mullen et al., 2015). In the second step, the data was decomposed using an adaptive mixture independent component analysis

(AMICA) (Palmer, J. A. et al., 2012) with the 'PCA keep option' to reduce the data rank to account for the number of interpolated channels. Subsequently, artefactual components were identified and removed using the Multiple Artifact Rejection Algorithm (MARA) (Winkler et al., 2011) in conjunction with visual inspection.

The data was then analysed using the FieldTrip toolbox for EEG/MEG analysis (Oostenveld, Fries, Maris, & Schoffelen, 2011). For the adjacency (connectivity) matrix estimation, 21 electrodes that have been shown to represent the activity of the frontoparietal regions were selected from the 128 electrodes to construct the brain network (Rojas et al., 2018). The preprocessed data was then segmented into 10second long segments, and approximately 10 of these 10second segments were analysed per participant. Based on the 10second long segments, the coherence (Coh) was utilized as a measure of the interactions between two electrodes. Coh is the most typically utilized method for analysing synchrony-defined cortical neuronal assemblies (Van Diessen et al., 2015). It represents the linear relationship at a specific frequency between two signals, $x(t)$ and $y(t)$, based on their cross-spectrum. Coh is expressed as follows:

$$C_{XY}(f) = \frac{|P_{XY}(f)|^2}{P_{XX}(f)P_{YY}(f)}$$

where $P_{XY}(f)$is the cross-spectrum of $x(t)$ and $y(t)$ at frequency f, and $P_{XX}(f)$and $P_{YY}(f)$ represent the auto spectrum at frequency f, as estimated from the Welch-based spectrum. Based on the frequency-dependent Coh, $C_{XY}(f)$, the edge linkages were calculated by averaging the Coh strength within the whole frequency band. After the paired Coh between each pair of 21 electrodes was calculated, the 21 × 21 weighted

adjacency (connectivity) matrix was constructed to represent the interactions among the 21 nodes for each segment in each participant. The adjacency (connectivity) matrices were then averaged across segments to achieve the final adjacency matrix for each participant. Finally, the brain network was constructed based on the 21 × 21 weighted adjacency (connectivity) matrix using the corresponding Coh as the edge linkage, w_{ij}, between two nodes, i and j.

Resting-State Network Properties

After the weighted network was constructed, the local and global efficiency metrics was calculated separately for each participant using the brain connectivity toolbox extension (Rubinov & Sporns, 2010). Here w_{ij} represents the connection strength between node *i* and node *j*, d_{ij} represent the *L* (i.e., shortest path length) between node i and node *j*, *N* represent the node number, and Θ represent the set of all nodes of a resting-state network. Global efficiency is defined as the inverse of the characteristic path length, where the characteristic path length is defined as the average shortest path length between all pairs of nodes in the network (Rubinov & Sporns, 2010). Global efficiency provides an estimate of a network's capacity for parallel information transfer and integrated processing among distributed components of the network (Latora & Marchiori, 2001; Watts & Strogatz, 1998). Global efficiency is calculated as follows:

$$Ge = \frac{1}{N}\sum_{i\in\Theta}\frac{\sum_{j\in\Theta,j\neq i}d_{ij}^{-1}}{N-1}$$

Local efficiency is a measure of the average efficiency of information transfer within a local subgraph (Rubinov & Sporns, 2010). The local efficiency of the network reveals how effectively information is transferred among the first neighbors of node i when node i is removed from the network (Latora & Marchiori, 2001; Watts & Strogatz, 1998). If neighbouring nodes are highly clustered the flow of information is more segregated and the network is more resilient (Betzel et al., 2014; Sporns & Honey, 2006). In the current study, local efficiency was averaged across the entire network. Local efficiency is calculated as follows:

$$Le = \frac{1}{N}\sum_{i\in\Theta}\frac{\sum_{j,l\in\Theta,j\neq i}\left(w_{ij}w_{il}\left[d_{jl}(\Theta_i)\right]^{-1}\right)^{1/3}}{\sum_{j\in\Theta}w_{ij}\left(\sum_{j\in\Theta}w_{ij}-1\right)}$$

ERP Data

See chapter 2 methodology section for data collection and processing details.

Results

Independent sample t-tests revealed that there was a significant age-related decline to both the global, $t(48) = 5.27$, $p < 0.01$, and local efficiency, $t(48) = 3.63$, $p < 0.01$of the frontoparietal network (see Figure 11).

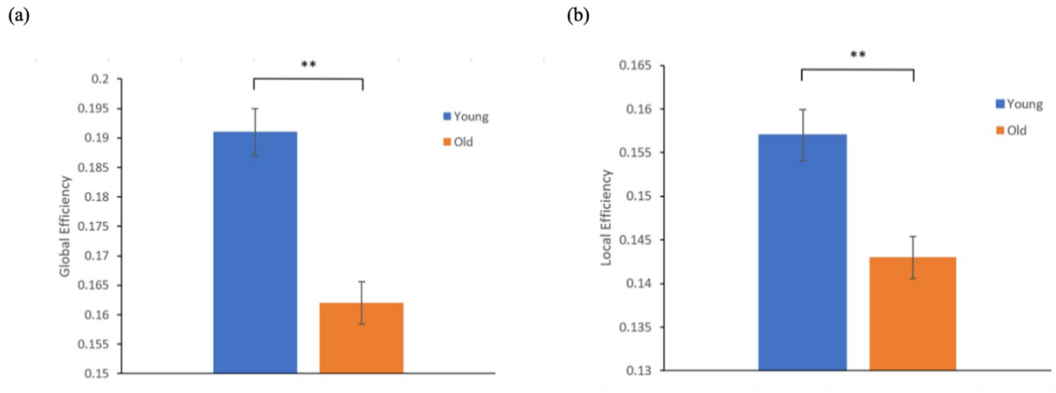

Figure 11. Global efficiency and (b) Local Efficiency for both older and younger participants. Error bars reflect standard error of the mean. ** = $p < .01$.

Subsequently, Pearson's correlation analysis was used to examine the relationship between the local and global efficiency of the frontoparietal network and the amplitude and latency of both the P3a and P3b, in younger and older adults (see Tables 2, 3, 4, and 5). We found a significant correlation between the global efficiency of the frontoparietal network and the amplitude of the P3b at electrode Fz in both younger and older adults. In younger adults, P3b amplitude (Fz) was negatively correlated to the global efficiency of the frontoparietal network. Conversely, in older adults P3b amplitude (Fz) was positively corelated to the global efficiency of the frontoparietal network. There was no evidence of any other significant relationships between either local or global efficiency and amplitude and/or latency of the P3a/P3b in either age group. There was also no correlation between either local or global efficiency and any behavioural measures.

Table 2

Correlation between global efficiency and P3a.

		P3a					
		Fz		Cz		Pz	
		Amplitude	Latency	Amplitude	Latency	Amplitude	Latency
Global Efficiency	Young	0.083 [-.323 .403]	0.096 [-.310 .474]	0.2 [-.212 .551]	0.21 [-.202 .559]	0.32 [-.086 .635]	-0.01 [-.403 .387]
	Old	0.031 [-.368 .421]	0.06 [-.343 .445]	0.308 [-.100 .627]	0.08 [-.325 .461]	0.333 [-.071 .644]	-0.031 [-.421 .368]

Table 3

Correlation between global efficiency and P3b.

		P3b					
		Fz		Cz		Pz	
		Amplitude	Latency	Amplitude	Latency	Amplitude	Latency
Global Efficiency	Young	**-0.505**** [-.750 -.137]	-0.247 [-.585 .164]	0.033 [-.367 .423]	0.257 [-.154 .592]	0.315 [-.092 .631]	-0.271 [-.602 .139]
	Old	**0.507**** [.140 .752]	-0.258 [-.593 .152]	-0.009 [-.402 .388]	0.241 [-170 .581]	0.093 [-.314 .471]	-0.251 [-.588 .160]

Note. Bolded items are significant at p<.01

Table 4

Correlation between local efficiency and P3a.

		P3a					
		Fz		Cz		Pz	
		Amplitude	Latency	Amplitude	Latency	Amplitude	Latency
Local Efficiency	Young	-0.121 [-.493 .288]	0.353 [-.049 .657]	-0.092 [-.470 .315]	0.196 [-.216 .549]	0.226 [-.186 .570]	0.091 [-.316 .469]
	Old	-0.04 [-.429 .361]	0.015 [-.382 .408]	0.238 [-.174 .578]	0.034 [-.366 .424]	0.399 [.005 .686]	-0.08 [-.460 .326]

Table 5

Correlation between local efficiency and P3b.

		P3b					
		Fz		Cz		Pz	
		Amplitude	Latency	Amplitude	Latency	Amplitude	Latency
Local Efficiency	Young	-0.366 [-.665 .034]	-0.161 [-.523 .250]	-0.076 [-.458 .329]	0.291 [-.110 .616]	0.28 [-.129 .608]	-0.131 [-.500 .279]
	Old	0.446 [.062 .715]	-0.22 [-.566 .191]	0.042 [-.359 .430]	0.313 [-.094 .630]	0.164 [-.247 .525]	-0.28 [-.094 .630]

Discussion

The goal of the third experimental chapter was to examine the age-related changes to the intrinsic efficiency of the frontoparietal network. Our results revealed a significant age-related decline to both global (loss of long-range pathways and longer average path length) and local efficiency (longer average path length between neighbouring nodes) within the frontoparietal network, which suggests that there are significant age-related declines to the frontoparietal network's ability to transmit information at both a global and local level (Latora & Marchiori, 2001; Rubinov & Sporns, 2010). Our results closely mirror the findings from previous studies which show significant age-related declines to the intrinsic connectivity of several large-scale neural networks including the default mode network (DMN), the dorsal attention network (DAN), the ventral attention network (VAN), and the frontoparietal control network (FPCN) (Geerligs, Renken, Saliasi, Maurits, & Lorist, 2015; Hausman et al., 2020; Onoda, Ishihara, & Yamaguchi, 2012; Onoda & Yamaguchi, 2013).

The decline in intrinsic network efficiency is hypothesized to be the result of significant age-related declines to the microstructural integrity of white matter pathways which reduces the network's efficiency by reducing the absolute amount of information that can be transmitted across the network, and also by causing significant rerouting of information (Bennett, Motes, Rao, & Rypma, 2012; Bennett & Madden, 2014; Honey et al., 2009; Madden et al., 2009; Madden et al., 2012). Additionally, the age-related decreases in dopamine concentration, dopamine receptor density, and transporter availability within the PFC (Bäckman et al., 2006; Bäckman et al., 2010; Kaasinen et al., 2000), reduces the stability of neural signalling within the frontoparietal network causing a reduction in network connectivity, by reducing the signal-to-noise ratio within the

network (Bäckman et al., 2006; Bäckman et al., 2010; Shafiei et al., 2019; Volkow et al., 2000).

However, despite the clear association between aging and decreased intrinsic connectivity within these large-scale neural networks, it is not yet clear how these changes contribute towards the cognitive aging process (Fleck et al., 2017; Hausman et al., 2020). For instance, several studies have shown that age-related declines to intrinsic connectivity within the DMN, FPCN, and VAN are linked to age-related declines in memory, executive function, and processing speed (Andrews-Hanna et al., 2007; Damoiseaux et al., 2008; Shaw, Schultz, Sperling, & Hedden, 2015). However, other studies have found either no evidence, or only limited evidence of a relationship between intrinsic connectivity declines and cognitive performance in older adults (Geerligs et al., 2015; Hausman et al., 2020; Onoda et al., 2012). This suggests that there is still a lot that we do not understand about the relationship between age-related changes to intrinsic connectivity and cognitive performance in older adults. Even in younger adults the relationship between the level of intrinsic connectivity within these large-scale networks and cognitive performance on tasks dependant on the network is not always clear (Parks & Madden, 2013). Therefore, in the current chapter, we explored how the intrinsic efficiency of the frontoparietal network relates to the generation of the P3a and P3b in both younger and older adults. Given the importance of global efficiency for the integration of information across the network, we predicted that global efficiency would be significantly correlated with the amplitude of the P3a and P3b at all midline electrode sites. However, we found that global efficiency was only related to the amplitude of the P3b at electrode Fz. Since, the amplitude of ERP components at a given electrode site is proposed to reflect the amount of neural resources engaged at that location, our results suggest that older adults with a higher level of global efficiency dedicate more frontal

resources towards the processing of target stimuli, while in younger adults' higher global efficiency results in a lower need to dedicate frontal resources to target stimuli and the ability to relegate processing to the more posterior regions. This however should be interpreted with caution as there was no significant relationship between global efficiency and P3b amplitude at posterior electrode sites in younger adults. Additionally, we also did not find any significant relationship between either local or global efficiency and latency of the P3a and P3b components, suggesting that intrinsic network efficiency may be more closely related to the quality of information transfer rather than the speed of information transfer. Overall, the results from the current study suggest that age-related changes to the efficiency of a network may impact its ability to function effectively and affect performance on tasks reliant on the network.

However, it is also important to remember that although the intrinsic connectivity of a network closely reflects the structural integrity of the network, it only provides an upper limit on the amount of information that can be transferred across the network, but does not show how effectively the network is being engaged in response to task demands (Honey et al., 2009). It may therefore also be important to explore how the network dynamically reconfigures in response to task demands (i.e., how the network topology shifts when participants transition from the resting-state phase to when they are actively engaged in a task) (Stanley et al., 2015). The ability of the network to dynamically reconfigure in response to task demands is critically dependent on the network's ability to flexibly shift between connectivity states characterized by higher integration or higher segregation depending on what is necessary at any given point (Deery et al., 2021; Michel & Koenig, 2018; Tang, Rothbart, & Posner, 2012). Unfortunately, recent studies examining the age-related changes to dynamic functional connectivity have shown that there is an age-related change to the nature and speed of transition between connectivity

states (Deery et al., 2021). Specifically, older adults exhibit a lower number of transitions between states of higher integration or higher segregation, and are also slower to transition between these states (Chen, Chou, Song, & Madden, 2009; Tian, Li, Wang, & Yu, 2018; Viviano, Raz, Yuan, & Damoiseaux, 2017). On the whole, these studies show that dynamic functional connectivity becomes less efficient and more random with age, making it more challenging to effectively engage the relevant networks in response to task demands (Battaglia et al., 2020; Ezaki, Sakaki, Watanabe, & Masuda, 2018; Tian et al., 2018), and also makes it more difficult to efficiently switch between tasks (Gold, Powell, Xuan, Jicha, & Smith, 2010; Jimura & Braver, 2010; Jolly et al., 2017). Given the considerable evidence that the brain actively fluctuates between periods of higher integration or segregation even during rest (Michel & Koenig, 2018; Tang et al., 2012), it would be beneficial to also examine the relationship between dynamic functional connectivity of the frontoparietal network at rest and the amplitude and/or latency of the P3a and P3b in future.

Chapter 5: General Discussion

Over the last 40 years, many studies have shown significant age-related changes to the amplitude, latency and topography of the P3a and P3b (Brown, Marsh, & LaRue, 1983; Fein & Turetsky, 1989; Fjell & Walhovd, 2001; Fjell & Walhovd, 2003; Fjell & Walhovd, 2004; Fjell et al., 2005; Fjell & Walhovd, 2005a; Fjell & Walhovd, 2005b; Fjell et al., 2007; Fjell et al., 2009; Walhovd & Fjell, 2003; Walhovd et al., 2008). In the current thesis, we focused on examining the age-related changes to the underlying neural dynamics responsible for these age-related changes to the P3a and P3b.

Our results revealed a significant age-related decline to both global and local efficiency within the frontoparietal network, which suggests that there are significant age-related declines to the frontoparietal network's ability to transmit information at both a global and local level (Latora & Marchiori, 2001; Rubinov & Sporns, 2010). The decline in intrinsic network efficiency is hypothesized to be the result of significant age-related declines to the microstructural integrity of white matter pathways which reduces the network's efficiency by reducing the absolute amount of information that can be transmitted across the network, and also by causing significant rerouting of information (Bennett et al., 2012; Bennett & Madden, 2014; Honey et al., 2009; Madden et al., 2009; Madden et al., 2012). Additionally, there are significant age-related declines to grey matter volume within the prefrontal, parietal and cingulate cortices (Farokhian, Yang, Beheshti, Matsuda, & Wu, 2017; Giorgio et al., 2010; Jernigan et al., 2001; Resnick, Pham, Kraut, Zonderman, & Davatzikos, 2003) caused by shrinkage of neurons (Peters, 2006) and microvascular pathology (Farkas & Luiten, 2001; Peters, 2006).

The age-related changes to the integrity of the frontoparietal network significantly affect the way older adults' perceive and respond to the presentation of unexpectedly

presented stimuli. These changes include an overall reduction in the amount of resources available for processing the oddball stimuli as reflected by the overall reduction to the amplitude of the P3a and P3b. It also reduces the speed with which older adults can process these stimuli as reflected by the prolongation of both P3a and P3b latency. But perhaps more importantly, there are significant age-related changes to the topography of the P3a and P3b which reflect the age-related changes to the way the brain processes these unexpectedly presented stimuli. The age-related increase to frontocentral theta-band activity during the T4 window aligns with the increase in amplitude of the P3a and P3b at electrode Fz, suggesting that the 'anterior-shift' of these components is caused by the increased dedication of attentional resources towards the processing of unexpectedly presented stimuli.

Although the 'anterior-shift' of the P3a and P3b were both caused by the increased allocation of attentional resources, the causal mechanisms underlying the shift were different in each case. More specifically, the 'anterior-shift' of the P3a was caused by an increase of feedforward connectivity from the dACC to DLPFC. This increase suggests that the older adults perceive the distractor as more surprising leading to the increase in resources dedicated to context updating purposes (seen in chapter 2). In contrast, the 'anterior-shift' of the P3b is caused by an increase modulation of feedback connection from the right DLPFC to the right IPS, and from the right IPS to the right MOG. This suggests that older adults' demonstrated an increased reliance on frontally-mediated control mechanisms to compensate for the increased difficulty in distinguishing between target and standard stimuli. The proposal that older adults had a more difficult time distinguishing between target and standard stimuli stems from both the weakening of feedforward connections (seen in chapter 3), as well as, the age-related decrease in centroparietal delta-band activity in response to target stimuli (seen in chapter 2).

It is evident that there are significant age-related changes to the efficiency of the frontoparietal network, there was also clear evidence of age-related changes to the P3a and P3b. In chapter 4, we examined the relationship between the age-related changes to the intrinsic functional connectivity of the frontoparietal network and the age-related changes to the amplitude and latency of the P3a and P3b. Given the importance of global efficiency for the integration of information across the network, we predicted that global efficiency would be significantly correlated with the amplitude and/or latency of the P3a and P3b at all midline electrode sites. However, we found that global efficiency was only related to the amplitude of the P3b at electrode Fz. Since, the amplitude of ERP components at a given electrode site is proposed to reflect the amount of neural resources engaged at that location, our results suggest that older adults with a higher level of global efficiency dedicate more frontal resources towards the processing of target stimuli. This supports the earlier proposal that the increased dedication of attentional resources towards target stimuli is a compensatory response to age-related perceptual and/or posterior cortical declines, and the ability to engage these compensatory mechanisms depend on the health and fitness of the frontoparietal network. In contrast, the increased allocation of attentional resources towards distractors is not related to the integrity of the frontoparietal network. Additionally, we also did not find any significant relationship between either local or global efficiency and latency of the P3a and P3b components. This is not surprising given the numerous other studies that have found either no evidence, or only limited evidence of a relationship between intrinsic connectivity declines and cognitive performance in older adults (Geerligs et al., 2015; Hausman et al., 2020; Onoda et al., 2012). This suggests that there is still a lot that we do not understand about the relationship between age-related changes to intrinsic connectivity and cognitive performance in older adults.

Limitations & Future Directions

One issue with examining the relationship between the age-related changes to intrinsic functional connectivity of the frontoparietal network and the age-related changes to the amplitude and latency of the P3a and P3b is that although the age-related changes to intrinsic functional connectivity closely reflects the age-related changes to the structural integrity of the network, it does not show us how effectively the network is engaged in response to task demands (Honey et al., 2009). It is therefore also important to explore how the network dynamically reconfigures in response to task demands (i.e., how the network topology shifts when participants transition from the resting-state phase to when they are actively engaged in a task) (Stanley et al., 2015). Additionally, it is also important to examine how the ability to dynamically reconfigure the network in response to task demands relates to key variables such as intellectual capacity, age and gender in order to partial out the variance not attributable to ageing. Unfortunately, using a brief screening tool only allowed us to exclude participants with clear signs of dementia but did not allow us to exclude participants with signs of mild cognitive impairment, it also did not allow us to assess participants' intellectual capacity. In future, a more extensive screening of participants cognitive status is needed in order to help tease apart the neural changes that are associated with successful cognitive aging from those that are associated with cognitive decline.

Beyond examining the age-related changes to the integrity of the frontoparietal network, it is also critical for us to examine the age-related changes to neurotransmitter systems involved in the generation of the P3a and P3b. For example, dopamine is important for stabilizing working memory representations (Durstewitz, Seamans, & Sejnowski, 2000; Eriksson, Vogel, Lansner, Bergström, & Nyberg, 2015), and is believed to be critical for the generation of the P3a (Warren, Kroll, & Kopp, 2023). Unfortunately,

considerable evidence suggests that a significant proportion of dopaminergic cells are lost between the ages of fifty and ninety (Carlsson & Winblad, 1976), with some estimates suggesting a loss of between 4-14% of receptors per decade (Karrer, Josef, Mata, Morris, & Samanez-Larkin, 2017). In addition, there is evidence that the dopaminergic system becomes less responsive as we age and older adults may require higher levels of presynaptic action (i.e., more intense cognitive stimulation) to elicit a similar level of postsynaptic activation when compared to younger adults (Riekmann & Nyberg, 2020). Similarly, noradrenaline plays an important role in the generation of the P3b, and age-related declines to noradrenaline may affect the generation of the P3b (Warren et al., 2023). To be clear, we need to not only study how the age-related changes to structural integrity and functional connectivity patterns influence the generation of the P3a and P3b, we also need to examine how the age-related changes to neurotransmitter systems, as well as, the age-related changes to other cellular and molecular mechanisms such as mitochondrial dysfunction, dysregulated glucose metabolism, dysregulated neuronal calcium homeostasis and increased inflammation affect the generation of the P3a and P3b in older adults (Mattson & Arumugam, 2018; Ridderinkhof & Krugers, 2022). Ultimately, having a more comprehensive assessment of the age-related microscopic to cellular and molecular mechanisms combined with an assessment of the macroscopic changes to the frontoparietal network will help provide better insights into the age-related changes to target and distractor processing.

Conclusion

In conclusion, the current thesis shows that there is a significant increase to the amount of attentional resources dedicated towards the processing of oddball stimuli, and the network dynamics responsible for the generation of the P3a and P3b changes as we age resulting in the ‘anterior-shift’ of the P3a and P3b that is seen across numerous

studies (Alperin et al., 2014; Friedman et al., 1993; O'Connell et al., 2012; West et al., 2010). However, the nature of this change is different for the P3a and P3b. For the P3a, the 'anterior-shift' appears to be caused by a failure to habituate towards the repeated presentation of oddball stimuli which causes a larger orienting response towards the distractor when it is presented (Richardson et al., 2011). In contrast, the 'anterior-shift' of the P3b appears to stem from a compensatory engagement of prefrontal areas to compensate for the reduced activity in posterior cortical regions caused by age-related sensory declines (O'Connell et al., 2012). Furthermore, these changes are caused by age-related changes to the frontoparietal network, although a clear relationship between the intrinsic functional connectivity and the generation of the P3a and P3b was not established. This simply suggests that the relationship between intrinsic functional connectivity changes and age-related changes to target and distractor processing are a little more complex and requires further investigation.

References

Ademoglu, A., Demiralp, T., Yordanova, J., Kolev, V., & Devrim, M. (1998). Decomposition of event-related brain potentials into multicomponents using wavelet transform. *Applied Signal Processing, 5*(3), 142-151.

Alperin, B. R., Mott, K. K., Rentz, D. M., Holcomb, P. J., & Daffner, K. R. (2014). Investigating the age-related "anterior shift" in the scalp distribution of the P3b component using principal component analysis. *Psychophysiology, 51*(7), 620-633.

Andrews-Hanna, J. R., Snyder, A. Z., Vincent, J. L., Lustig, C., Head, D., Raichle, M. E., & Buckner, R. L. (2007). Disruption of large-scale brain systems in advanced aging. *Neuron, 56*(5), 924-935.

Ardekani, B. A., Choi, S. J., Hossein-Zadeh, G., Porjesz, B., Tanabe, J. L., Lim, K. O., . . . Begleiter, H. (2002). Functional magnetic resonance imaging of brain activity in the visual oddball task. *Cognitive Brain Research, 14*(3), 347-356.

Arrington, C. M., Carr, T. H., Mayer, A. R., & Rao, S. M. (2000). Neural mechanisms of visual attention: Object-based selection of a region in space. *Journal of Cognitive Neuroscience, 12*(Supplement 2), 106-117.

Bachman, M. D., & Bernat, E. M. (2018). Independent contributions of theta and delta time-frequency activity to the visual oddball P3b. *International Journal of Psychophysiology, 128*, 70-80.

Bäckman, L., Lindenberger, U., Li, S., & Nyberg, L. (2010). Linking cognitive aging to alterations in dopamine neurotransmitter functioning: Recent data and future avenues. *Neuroscience & Biobehavioral Reviews, 34*(5), 670-677.

Bäckman, L., Nyberg, L., Lindenberger, U., Li, S., & Farde, L. (2006). The correlative triad among aging, dopamine, and cognition: Current status and future prospects. *Neuroscience & Biobehavioral Reviews, 30*(6), 791-807.

Barrett, G., Neshige, R., & Shibasaki, H. (1987). Human auditory and somatosensory event-related potentials: Effects of response condition and age. *Electroencephalography and Clinical Neurophysiology, 66*(4), 409-419.

Basar, E. (1980). Relation between EEG and brain evoked potentials. *EEG-Brain Dynamics,*

Başar, E., Başar-Eroglu, C., Karakaş, S., & Schürmann, M. (2001). Gamma, alpha, delta, and theta oscillations govern cognitive processes. *International Journal of Psychophysiology, 39*(2-3), 241-248.

Başar, E., & Güntekin, B. (2012). A short review of alpha activity in cognitive processes and in cognitive impairment. *International Journal of Psychophysiology, 86*(1), 25-38.

Başar-Eroglu, C., Başar, E., Demiralp, T., & Schürmann, M. (1992). P300-response: Possible psychophysiological correlates in delta and theta frequency channels. A review. *International Journal of Psychophysiology, 13*(2), 161-179.

Bassett, D. S., & Sporns, O. (2017). Network neuroscience. *Nature Neuroscience, 20*(3), 353-364.

Battaglia, D., Boudou, T., Hansen, E. C., Lombardo, D., Chettouf, S., Daffertshofer, A., . . . Jirsa, V. (2020). Dynamic functional connectivity between order and randomness and its evolution across the human adult lifespan. *NeuroImage, 222*, 117156.

Baudena, P., Halgren, E., Heit, G., & Clarke, J. M. (1995). Intracerebral potentials to rare target and distractor auditory and visual stimuli. III. frontal cortex. *Electroencephalography and Clinical Neurophysiology, 94*(4), 251-264.

Bennett, I. J., & Madden, D. J. (2014). Disconnected aging: Cerebral white matter integrity and age-related differences in cognition. *Neuroscience, 276*, 187-205.

Bennett, I. J., Motes, M. A., Rao, N. K., & Rypma, B. (2012). White matter tract integrity predicts visual search performance in young and older adults. *Neurobiology of Aging, 33*(2), 433. e21-433. e31.

Bernat, E. M., Williams, W. J., & Gehring, W. J. (2005). Decomposing ERP time–frequency energy using PCA. *Clinical Neurophysiology, 116*(6), 1314-1334.

Betzel, R. F., Byrge, L., He, Y., Goñi, J., Zuo, X., & Sporns, O. (2014). Changes in structural and functional connectivity among resting-state networks across the human lifespan. *NeuroImage, 102*, 345-357.

Bledowski, C., Prvulovic, D., Goebel, R., Zanella, F. E., & Linden, D. E. (2004). Attentional systems in target and distractor processing: A combined ERP and fMRI study. *NeuroImage, 22*(2), 530-540.

Bledowski, C., Prvulovic, D., Hoechstetter, K., Scherg, M., Wibral, M., Goebel, R., & Linden, D. E. (2004). Localizing P300 generators in visual target and distractor processing: A combined event-related potential and functional magnetic resonance imaging study. *Journal of Neuroscience, 24*(42), 9353-9360.

Bocquillon, P., Bourriez, J., Palmero-Soler, E., Betrouni, N., Houdayer, E., Derambure, P., & Dujardin, K. (2011). Use of swLORETA to localize the cortical sources of

target-and distracter-elicited P300 components. *Clinical Neurophysiology, 122*(10), 1991-2002.

Botvinick, M. M., Cohen, J. D., & Carter, C. S. (2004). Conflict monitoring and anterior cingulate cortex: An update. *Trends in Cognitive Sciences, 8*(12), 539-546.

Botvinick, M., Nystrom, L. E., Fissell, K., Carter, C. S., & Cohen, J. D. (1999). Conflict monitoring versus selection-for-action in anterior cingulate cortex. *Nature, 402*(6758), 179-181.

Brainard, D. H., & Vision, S. (1997). The psychophysics toolbox. *Spatial Vision, 10*(4), 433-436.

Bramon, E., Rabe-Hesketh, S., Sham, P., Murray, R. M., & Frangou, S. (2004). Meta-analysis of the P300 and P50 waveforms in schizophrenia. *Schizophrenia Research, 70*(2-3), 315-329.

Braver, T. S., & Barch, D. M. (2002). A theory of cognitive control, aging cognition, and neuromodulation. *Neuroscience & Biobehavioral Reviews, 26*(7), 809-817.

Bressler, S. L., Tang, W., Sylvester, C. M., Shulman, G. L., & Corbetta, M. (2008). Top-down control of human visual cortex by frontal and parietal cortex in anticipatory visual spatial attention. *Journal of Neuroscience, 28*(40), 10056-10061.

Brown, W. S., Marsh, J. T., & LaRue, A. (1983). Exponential electrophysiological aging: P3 latency. *Electroencephalography and Clinical Neurophysiology, 55*(3), 277-285.

Buzsáki, G., & Wang, X. (2012). Mechanisms of gamma oscillations. *Annual Review of Neuroscience, 35*, 203.

Cabeza, R., Anderson, N. D., Locantore, J. K., & McIntosh, A. R. (2002). Aging gracefully: Compensatory brain activity in high-performing older adults. *NeuroImage, 17*(3), 1394-1402.

Campbell, K. L., Grady, C. L., Ng, C., & Hasher, L. (2012). Age differences in the frontoparietal cognitive control network: Implications for distractibility. *Neuropsychologia, 50*(9), 2212-2223.

Carlsson, A., & Winblad, B. (1976). Influence of age and time interval between death and autopsy on dopamine and 3-methoxytyramine levels in human basal ganglia. *Journal of Neural Transmission, 38*, 271-276.

Carter, C. S., & Van Veen, V. (2007). Anterior cingulate cortex and conflict detection: An update of theory and data. *Cognitive, Affective, & Behavioral Neuroscience, 7*(4), 367-379.

Chang, C., Hsu, S., Pion-Tonachini, L., & Jung, T. (2018). Evaluation of artifact subspace reconstruction for automatic EEG artifact removal. Paper presented at the *2018 40th Annual International Conference of the IEEE Engineering in Medicine and Biology Society (EMBC),* 1242-1245.

Chen, N., Chou, Y., Song, A. W., & Madden, D. J. (2009). Measurement of spontaneous signal fluctuations in fMRI: Adult age differences in intrinsic functional connectivity. *Brain Structure and Function, 213*(6), 571-585.

Chun, M. M., Golomb, J. D., & Turk-Browne, N. B. (2011). A taxonomy of external and internal attention. *Annual Review of Psychology, 62*, 73-101.

Cipolotti, L., Healy, C., Chan, E., Bolsover, F., Lecce, F., White, M., . . . Bozzali, M. (2015). The impact of different aetiologies on the cognitive performance of frontal patients. *Neuropsychologia, 68*, 21-30.

Clark, V. P., Fannon, S., Lai, S., Benson, R., & Bauer, L. (2000). Responses to rare visual target and distractor stimuli using event-related fMRI. *Journal of Neurophysiology, 83*(5), 3133-3139.

Clayton, M. S., Yeung, N., & Kadosh, R. C. (2015). The roles of cortical oscillations in sustained attention. *Trends in Cognitive Sciences, 19*(4), 188-195.

Cohen, M. X. (2014). *Analyzing neural time series data: Theory and practice* MIT press.

Comerchero, M. D., & Polich, J. (1999). P3a and P3b from typical auditory and visual stimuli. *Clinical Neurophysiology, 110*(1), 24-30.

Corbetta, M., Patel, G., & Shulman, G. L. (2008). The reorienting system of the human brain: From environment to theory of mind. *Neuron, 58*(3), 306-324.

Corbetta, M., & Shulman, G. L. (2002). Control of goal-directed and stimulus-driven attention in the brain. *Nature Reviews Neuroscience, 3*(3), 201-215.

Courchesne, E., Hillyard, S. A., & Galambos, R. (1975). Stimulus novelty, task relevance and the visual evoked potential in man. *Electroencephalography and Clinical Neurophysiology, 39*(2), 131-143.

Daffner, K. R., Mesulam, M. M., Scinto, L., Acar, D., Calvo, V., Faust, R., . . . Holcomb, P. (2000). The central role of the prefrontal cortex in directing attention to novel events. *Brain, 123*(5), 927-939.

Daffner, K. R., Ryan, K. K., Williams, D. M., Budson, A. E., Rentz, D. M., Scinto, L. F., & Holcomb, P. J. (2005). Age-related differences in novelty and target processing among cognitively high performing adults. *Neurobiology of Aging, 26*(9), 1283-1295.

Daffner, K. R., Ryan, K. K., Williams, D. M., Budson, A. E., Rentz, D. M., Wolk, D. A., & Holcomb, P. J. (2006). Age-related differences in attention to novelty among cognitively high performing adults. *Biological Psychology, 72*(1), 67-77.

Damoiseaux, J. S. (2017). Effects of aging on functional and structural brain connectivity. *NeuroImage, 160*, 32-40.

Damoiseaux, J. S., Beckmann, C. F., Arigita, E. S., Barkhof, F., Scheltens, P., Stam, C. J., . . . Rombouts, S. (2008). Reduced resting-state brain activity in the "default network" in normal aging. *Cerebral Cortex, 18*(8), 1856-1864.

Daubechies, I. (1990). The wavelet transform, time-frequency localization and signal analysis. *IEEE Transactions on Information Theory, 36*(5), 961-1005.

David, O., & Friston, K. J. (2003). A neural mass model for MEG/EEG:: Coupling and neuronal dynamics. *NeuroImage, 20*(3), 1743-1755.

David, O., Kiebel, S. J., Harrison, L. M., Mattout, J., Kilner, J. M., & Friston, K. J. (2006). Dynamic causal modeling of evoked responses in EEG and MEG. *NeuroImage, 30*(4), 1255-1272.

Davis, S. W., Dennis, N. A., Daselaar, S. M., Fleck, M. S., & Cabeza, R. (2008). Que PASA? the posterior–anterior shift in aging. *Cerebral Cortex, 18*(5), 1201-1209.

De Boor, C. (2005). *Spline toolbox for use with MATLAB: User's guide, version 3* MathWorks.

de Fockert, J. W., Ramchurn, A., Van Velzen, J., Bergström, Z., & Bunce, D. (2009). Behavioral and ERP evidence of greater distractor processing in old age. *Brain Research, 1282*, 67-73.

De Schotten, M. T., Dell'Acqua, F., Forkel, S., Simmons, A., Vergani, F., Murphy, D. G., & Catani, M. (2011). A lateralized brain network for visuo-spatial attention. *Nature Precedings,* , 1.

Debener, S., Makeig, S., Delorme, A., & Engel, A. K. (2005). What is novel in the novelty oddball paradigm? functional significance of the novelty P3 event-related potential as revealed by independent component analysis. *Cognitive Brain Research, 22*(3), 309-321.

Deery, H., Di Paolo, R., Moran, C., Egan, G., & Jamadar, S. (2021). The older adult brain is less modular, more integrated and less efficient at rest: A systematic review of large-scale resting-state functional brain networks across the adult lifespan.

Delorme, A., & Makeig, S. (2004). EEGLAB: An open source toolbox for analysis of single-trial EEG dynamics including independent component analysis. *Journal of Neuroscience Methods, 134*(1), 9-21.

Demiralp, T., & Ademoglu, A. (2001). Decomposition of event-related brain potentials into multiple functional components using wavelet transform. *Clinical Electroencephalography, 32*(3), 122-138.

Demiralp, T., Ademoglu, A., Comerchero, M., & Polich, J. (2001). Wavelet analysis of P3a and P3b. *Brain Topography, 13*(4), 251-267.

Desmurget, M., Bonnetblanc, F., & Duffau, H. (2007). Contrasting acute and slow-growing lesions: A new door to brain plasticity. *Brain, 130*(4), 898-914.

DiQuattro, N. E., & Geng, J. J. (2011). Contextual knowledge configures attentional control networks. *Journal of Neuroscience, 31*(49), 18026-18035.

Donchin, E. (1981). Surprise!… surprise? *Psychophysiology, 18*(5), 493-513.

Donchin, E., & Coles, M. G. (1988). Is the P300 component a manifestation of context updating? *Behavioral and Brain Sciences, 11*(3), 357-374.

Downar, J., Crawley, A. P., Mikulis, D. J., & Davis, K. D. (2000). A multimodal cortical network for the detection of changes in the sensory environment. *Nature Neuroscience, 3*(3), 277-283.

Downar, J., Crawley, A. P., Mikulis, D. J., & Davis, K. D. (2001). The effect of task relevance on the cortical response to changes in visual and auditory stimuli: An event-related fMRI study. *NeuroImage, 14*(6), 1256-1267.

Duffau, H. (2011). Do brain tumours allow valid conclusions on the localisation of human brain functions? *Cortex, 47*(8), 1016-1017.

Durstewitz, D., Seamans, J. K., & Sejnowski, T. J. (2000). Dopamine-mediated stabilization of delay-period activity in a network model of prefrontal cortex. *Journal of Neurophysiology,*

Eichele, T., Specht, K., Moosmann, M., Jongsma, M. L., Quiroga, R. Q., Nordby, H., & Hugdahl, K. (2005). Assessing the spatiotemporal evolution of neuronal activation with single-trial event-related potentials and functional MRI. *Proceedings of the National Academy of Sciences, 102*(49), 17798-17803.

Eriksson, J., Vogel, E. K., Lansner, A., Bergström, F., & Nyberg, L. (2015). Neurocognitive architecture of working memory. *Neuron, 88*(1), 33-46.

Escera, C., Alho, K., Winkler, I., & Näätänen, R. (1998). Neural mechanisms of involuntary attention to acoustic novelty and change. *Journal of Cognitive Neuroscience, 10*(5), 590-604.

Esquenazi, Y., Lo, V. P., & Lee, K. (2017). Critical care management of cerebral edema in brain tumors. *Journal of Intensive Care Medicine, 32*(1), 15-24.

Ezaki, T., Sakaki, M., Watanabe, T., & Masuda, N. (2018). A ge-related changes in the ease of dynamical transitions in human brain activity. *Human Brain Mapping, 39*(6), 2673-2688.

Fabiani, M., Friedman, D., & Cheng, J. C. (1998). Individual differences in P3 scalp distribution in older adults, and their relationship to frontal lobe function. *Psychophysiology, 35*(6), 698-708.

Fabiani, M., Low, K. A., Wee, E., Sable, J. J., & Gratton, G. (2006). Reduced suppression or labile memory? mechanisms of inefficient filtering of irrelevant information in older adults. *Journal of Cognitive Neuroscience, 18*(4), 637-650.

Falkenstein, M., Hoormann, J., & Hohnsbein, J. (1999). ERP components in go/nogo tasks and their relation to inhibition. *Acta Psychologica, 101*(2-3), 267-291.

Farkas, E., & Luiten, P. G. (2001). Cerebral microvascular pathology in aging and alzheimer's disease. *Progress in Neurobiology, 64*(6), 575-611.

Farokhian, F., Yang, C., Beheshti, I., Matsuda, H., & Wu, S. (2017). Age-related gray and white matter changes in normal adult brains. *Aging and Disease, 8*(6), 899.

Fein, G., & Turetsky, B. (1989). P300 latency variability in normal elderly: Effects of paradigm and measurement technique. *Electroencephalography and Clinical Neurophysiology, 72*(5), 384-394.

Felleman, D. J., & Van Essen, D. C. (1991). Distributed hierarchical processing in the primate cerebral cortex. Paper presented at the *Cereb Cortex,*

Ferree, T. C., Luu, P., Russell, G. S., & Tucker, D. M. (2001). Scalp electrode impedance, infection risk, and EEG data quality. *Clinical Neurophysiology, 112*(3), 536-544.

Filipović, S. R., & Kostić, V. S. (1995). Utility of auditory P300 in detection of presenile dementia. *Journal of the Neurological Sciences, 131*(2), 150-155.

Fjell, A. M., Rosquist, H., & Walhovd, K. B. (2009). Instability in the latency of P3a/P3b brain potentials and cognitive function in aging. *Neurobiology of Aging, 30*(12), 2065-2079.

Fjell, A. M., & Walhovd, K. B. (2001). P300 and neuropsychological tests as measures of aging: Scalp topography and cognitive changes. *Brain Topography, 14*(1), 25-40.

Fjell, A. M., & Walhovd, K. B. (2003). P3a and neuropsychological ‘Frontal’tests in aging. *Aging, Neuropsychology, and Cognition, 10*(3), 169-181.

Fjell, A. M., & Walhovd, K. B. (2004). Life-span changes in P3a. *Psychophysiology, 41*(4), 575-583.

Fjell, A. M., & Walhovd, K. B. (2005a). Age-sensitivity of P3 in high-functioning adults. *Neurobiology of Aging, 26*(9), 1297-1299.

Fjell, A. M., & Walhovd, K. B. (2005b). High versus average cognitive function: Implications for the age-sensitivity of P3.

Fjell, A. M., Walhovd, K. B., Fischl, B., & Reinvang, I. (2007). Cognitive function, P3a/P3b brain potentials, and cortical thickness in aging. *Human Brain Mapping, 28*(11), 1098-1116.

Fjell, A. M., Walhovd, K. B., & Reinvang, I. (2005). Age-dependent changes in distribution of P3a/P3b amplitude and thickness of the cerebral cortex. *Neuroreport, 16*(13), 1451-1454.

Fleck, J. I., Kuti, J., Mercurio, J., Mullen, S., Austin, K., & Pereira, O. (2017). The impact of age and cognitive reserve on resting-state brain connectivity. *Frontiers in Aging Neuroscience, 9*, 392.

Folstein, M. F., Robins, L. N., & Helzer, J. E. (1983). The mini-mental state examination. *Archives of General Psychiatry, 40*(7), 812.

Fox, M. D., Corbetta, M., Snyder, A. Z., Vincent, J. L., & Raichle, M. E. (2006). Spontaneous neuronal activity distinguishes human dorsal and ventral attention systems. *Proceedings of the National Academy of Sciences, 103*(26), 10046-10051.

Fox, M. D., & Raichle, M. E. (2007). Spontaneous fluctuations in brain activity observed with functional magnetic resonance imaging. *Nature Reviews Neuroscience, 8*(9), 700-711.

Fox, M. D., Snyder, A. Z., Vincent, J. L., Corbetta, M., Van Essen, D. C., & Raichle, M. E. (2005). The human brain is intrinsically organized into dynamic, anticorrelated functional networks. *Proceedings of the National Academy of Sciences, 102*(27), 9673-9678.

Friedman, D. (2003). Cognition and aging: A highly selective overview of event-related potential (ERP) data. *Journal of Clinical and Experimental Neuropsychology, 25*(5), 702-720.

Friedman, D., Cycowicz, Y. M., & Gaeta, H. (2001). The novelty P3: An event-related brain potential (ERP) sign of the brain's evaluation of novelty. *Neuroscience & Biobehavioral Reviews, 25*(4), 355-373.

Friedman, D., Kazmerski, V., & Fabiani, M. (1997). An overview of age-related changes in the scalp distribution of P3b. *Electroencephalography and Clinical Neurophysiology/Evoked Potentials Section, 104*(6), 498-513.

Friedman, D., Simpson, G., & Hamberger, M. (1993). Age-related changes in scalp topography to novel and target stimuli. *Psychophysiology, 30*(4), 383-396.

Friston, K. J. (2011). Functional and effective connectivity: A review. *Brain Connectivity, 1*(1), 13-36.

Friston, K. J., Harrison, L., & Penny, W. (2003). Dynamic causal modelling. *NeuroImage, 19*(4), 1273-1302.

Friston, K. J., Litvak, V., Oswal, A., Razi, A., Stephan, K. E., Van Wijk, B. C., . . . Zeidman, P. (2016). Bayesian model reduction and empirical bayes for group (DCM) studies. *NeuroImage, 128*, 413-431.

Friston, K., Zeidman, P., & Litvak, V. (2015). Empirical bayes for DCM: A group inversion scheme. *Frontiers in Systems Neuroscience, 9*, 164.

Gaillard, A. (1988). Problems and paradigms in ERP research. *Biological Psychology, 26*(1-3), 91-109.

Geerligs, L., Renken, R. J., Saliasi, E., Maurits, N. M., & Lorist, M. M. (2015). A brain-wide study of age-related changes in functional connectivity. *Cerebral Cortex, 25*(7), 1987-1999.

Giesbrecht, B., Woldorff, M. G., Song, A. W., & Mangun, G. R. (2003). Neural mechanisms of top-down control during spatial and feature attention. *NeuroImage, 19*(3), 496-512.

Giorgio, A., Santelli, L., Tomassini, V., Bosnell, R., Smith, S., De Stefano, N., & Johansen-Berg, H. (2010). Age-related changes in grey and white matter structure throughout adulthood. *NeuroImage, 51*(3), 943-951.

Gold, B. T., Powell, D. K., Xuan, L., Jicha, G. A., & Smith, C. D. (2010). Age-related slowing of task switching is associated with decreased integrity of frontoparietal white matter. *Neurobiology of Aging, 31*(3), 512-522.

Goodin, D. S., Squires, K. C., Henderson, B. H., & Starr, A. (1978). Age-related variations in evoked potentials to auditory stimuli in normal human subjects. *Electroencephalography and Clinical Neurophysiology, 44*(4), 447-458.

Halgren, E., Baudena, P., Clarke, J. M., Heit, G., Liégeois, C., Chauvel, P., & Musolino, A. (1995a). Intracerebral potentials to rare target and distractor auditory and visual stimuli. I. superior temporal plane and parietal lobe. *Electroencephalography and Clinical Neurophysiology, 94*(3), 191-220.

Halgren, E., Baudena, P., Clarke, J. M., Heit, G., Marinkovic, K., Devaux, B., . . . Biraben, A. (1995). Intracerebral potentials to rare target and distractor auditory and visual stimuli. II. medial, lateral and posterior temporal lobe. *Electroencephalography and Clinical Neurophysiology, 94*(4), 229-250.

Harper, J., Malone, S. M., & Iacono, W. G. (2017). Theta-and delta-band EEG network dynamics during a novelty oddball task. *Psychophysiology, 54*(11), 1590-1605.

Hausman, H. K., O'Shea, A., Kraft, J. N., Boutzoukas, E. M., Evangelista, N. D., Van Etten, E. J., . . . Hishaw, G. A. (2020). The role of resting-state network functional connectivity in cognitive aging. *Frontiers in Aging Neuroscience, 12*, 177.

He, B., Lian, J., Spencer, K. M., Dien, J., & Donchin, E. (2001). A cortical potential imaging analysis of the P300 and novelty P3 components. *Human Brain Mapping, 12*(2), 120-130.

Healey, M. K., Campbell, K. L., & Hasher, L. (2008). Cognitive aging and increased distractibility: Costs and potential benefits. *Progress in Brain Research, 169*, 353-363.

Hedges, D., Janis, R., Mickelson, S., Keith, C., Bennett, D., & Brown, B. L. (2016). P300 amplitude in alzheimer's disease: A meta-analysis and meta-regression. *Clinical EEG and Neuroscience, 47*(1), 48-55.

Hesselbrock, V., Begleiter, H., Porjesz, B., O'Connor, S., & Bauer, L. (2001). P300 event-related potential amplitude as an endophenotype of alcoholism–evidence from the collaborative study on the genetics of alcoholism. *Journal of Biomedical Science, 8*(1), 77-82.

Honey, C. J., Sporns, O., Cammoun, L., Gigandet, X., Thiran, J., Meuli, R., & Hagmann, P. (2009). Predicting human resting-state functional connectivity from structural connectivity. *Proceedings of the National Academy of Sciences, 106*(6), 2035-2040.

Indovina, I., & Macaluso, E. (2007). Dissociation of stimulus relevance and saliency factors during shifts of visuospatial attention. *Cerebral Cortex, 17*(7), 1701-1711.

Jeon, Y., & Polich, J. (2003). Meta-analysis of P300 and schizophrenia: Patients, paradigms, and practical implications. *Psychophysiology, 40*(5), 684-701.

Jernigan, T. L., Archibald, S. L., Fennema-Notestine, C., Gamst, A. C., Stout, J. C., Bonner, J., & Hesselink, J. R. (2001). Effects of age on tissues and regions of the cerebrum and cerebellum. *Neurobiology of Aging, 22*(4), 581-594.

Jimura, K., & Braver, T. S. (2010). Age-related shifts in brain activity dynamics during task switching. *Cerebral Cortex, 20*(6), 1420-1431.

Johnson Jr, R. (1989). Auditory and visual P300s in temporal lobectomy patients: Evidence for modality-dependent generators. *Psychophysiology, 26*(6), 633-650.

Johnson Jr, R. (1993). On the neural generators of the P300 component of the event-related potential. *Psychophysiology, 30*(1), 90-97.

Jolly, T. A., Cooper, P. S., Rennie, J. L., Levi, C. R., Lenroot, R., Parsons, M. W., . . . Karayanidis, F. (2017). Age-related decline in task switching is linked to both global and tract-specific changes in white matter microstructure. *Human Brain Mapping, 38*(3), 1588-1603.

Jørgensen, H. S., Nakayama, H., Raaschou, H. O., Vive-Larsen, J., Støier, M., & Olsen, T. S. (1995). Outcome and time course of recovery in stroke. part I: Outcome. the copenhagen stroke study. *Archives of Physical Medicine and Rehabilitation, 76*(5), 399-405.

Juckel, G., Karch, S., Kawohl, W., Kirsch, V., Jäger, L., Leicht, G., . . . Ertl, M. (2012). Age effects on the P300 potential and the corresponding fMRI BOLD-signal. *NeuroImage, 60*(4), 2027-2034.

Kaasinen, V., Vilkman, H., Hietala, J., Någren, K., Helenius, H., Olsson, H., . . . Rinne, J. O. (2000). Age-related dopamine D2/D3 receptor loss in extrastriatal regions of the human brain. *Neurobiology of Aging, 21*(5), 683-688.

Karrer, T. M., Josef, A. K., Mata, R., Morris, E. D., & Samanez-Larkin, G. R. (2017). Reduced dopamine receptors and transporters but not synthesis capacity in normal aging adults: A meta-analysis. *Neurobiology of Aging, 57*, 36-46.

Kiebel, S. J., David, O., & Friston, K. J. (2006). Dynamic causal modelling of evoked responses in EEG/MEG with lead field parameterization. *NeuroImage, 30*(4), 1273-1284.

Kiehl, K. A., Laurens, K. R., Duty, T. L., Forster, B. B., & Liddle, P. F. (2001). Neural sources involved in auditory target detection and novelty processing: An event-related fMRI study. *Psychophysiology, 38*(1), 133-142.

Kim, H. (2014). Involvement of the dorsal and ventral attention networks in oddball stimulus processing: A meta-analysis. *Human Brain Mapping, 35*(5), 2265-2284.

Kim, S., Hasher, L., & Zacks, R. T. (2007). Aging and a benefit of distractibility. *Psychonomic Bulletin & Review, 14*(2), 301-305.

Kincade, J. M., Abrams, R. A., Astafiev, S. V., Shulman, G. L., & Corbetta, M. (2005). An event-related functional magnetic resonance imaging study of voluntary and stimulus-driven orienting of attention. *Journal of Neuroscience, 25*(18), 4593-4604.

Kirino, E., Belger, A., Goldman-Rakic, P., & McCarthy, G. (2000). Prefrontal activation evoked by infrequent target and novel stimuli in a visual target detection task: An event-related functional magnetic resonance imaging study. *Journal of Neuroscience, 20*(17), 6612-6618.

Kleiner, M., Brainard, D., & Pelli, D. (2007). What's new in psychtoolbox-3?

Knight, R. T. (1984). Decreased response to novel stimuli after prefrontal lesions in man. *Electroencephalography and Clinical Neurophysiology/Evoked Potentials Section, 59*(1), 9-20.

Knight, R. T. (1996). Contribution of human hippocampal region to novelty detection. *Nature, 383*(6597), 256-259.

Knight, R. T., & Scabini, D. (1998). Anatomic bases of event-related potentials and their relationship to novelty detection in humans. *Journal of Clinical Neurophysiology, 15*(1), 3-13.

Knight, R. T., Scabini, D., Woods, D. L., & Clayworth, C. C. (1989). Contributions of temporal-parietal junction to the human auditory P3. *Brain Research, 502*(1), 109-116.

Koessler, L., Cecchin, T., Colnat-Coulbois, S., Vignal, J., Jonas, J., Vespignani, H., . . . Maillard, L. G. (2015). Catching the invisible: Mesial temporal source contribution to simultaneous EEG and SEEG recordings. *Brain Topography, 28*(1), 5-20.

Kolev, V., Demiralp, T., Yordanova, J., Ademoglu, A., & Isoglu-Alkaç, Ü. (1997). Time–frequency analysis reveals multiple functional components during oddball P300. *Neuroreport, 8*(8), 2061-2065.

Kutas, M., McCarthy, G., & Donchin, E. (1977). Augmenting mental chronometry: The P300 as a measure of stimulus evaluation time. *Science, 197*(4305), 792-795.

Lachaux, J. P., Rudrauf, D., & Kahane, P. (2003). Intracranial EEG and human brain mapping. *Journal of Physiology-Paris, 97*(4-6), 613-628.

Latora, V., & Marchiori, M. (2001). Efficient behavior of small-world networks. *Physical Review Letters, 87*(19), 198701.

Lemaréchal, J., George, N., & David, O. (2018). Comparison of two integration methods for dynamic causal modeling of electrophysiological data. *NeuroImage, 173*, 623-631.

Linden, D. E. (2005). The P300: Where in the brain is it produced and what does it tell us? *The Neuroscientist, 11*(6), 563-576.

Linden, D. E., Prvulovic, D., Formisano, E., Völlinger, M., Zanella, F. E., Goebel, R., & Dierks, T. (1999). The functional neuroanatomy of target detection: An fMRI study of visual and auditory oddball tasks. *Cerebral Cortex, 9*(8), 815-823.

Liu, T., Slotnick, S. D., Serences, J. T., & Yantis, S. (2003). Cortical mechanisms of feature-based attentional control. *Cerebral Cortex, 13*(12), 1334-1343.

Lopez-Calderon, J., & Luck, S. J. (2014). ERPLAB: An open-source toolbox for the analysis of event-related potentials. *Frontiers in Human Neuroscience, 8*, 213.

Lorenzo-López, L., Amenedo, E., Pazo-Álvarez, P., & Cadaveira, F. (2007). Visual target processing in high-and low-performing older subjects indexed by P3 component. *Neurophysiologie Clinique/Clinical Neurophysiology, 37*(2), 53-61.

Lorenzo-López, L., Amenedo, E., Pascual-Marqui, R. D., & Cadaveira, F. (2008). Neural correlates of age-related visual search decline: A combined ERP and sLORETA study. *NeuroImage, 41*(2), 511-524.

Luck, S. J. (2014). *An introduction to the event-related potential technique* MIT press.

Luck, S. J., Woodman, G. F., & Vogel, E. K. (2000). Event-related potential studies of attention. *Trends in Cognitive Sciences, 4*(11), 432-440.

Luu, P., & Ferree, T. (2005). Determination of the HydroCel geodesic sensor nets' average electrode positions and their 10–10 international equivalents. *Inc, Technical Note,* , 1-11.

Madden, D. J., Bennett, I. J., Burzynska, A., Potter, G. G., Chen, N., & Song, A. W. (2012). Diffusion tensor imaging of cerebral white matter integrity in cognitive aging. *Biochimica Et Biophysica Acta (BBA)-Molecular Basis of Disease, 1822*(3), 386-400.

Madden, D. J., Bennett, I. J., & Song, A. W. (2009). Cerebral white matter integrity and cognitive aging: Contributions from diffusion tensor imaging. *Neuropsychology Review, 19*(4), 415.

Madden, D. J., Spaniol, J., Whiting, W. L., Bucur, B., Provenzale, J. M., Cabeza, R., . . . Huettel, S. A. (2007). Adult age differences in the functional neuroanatomy of visual attention: A combined fMRI and DTI study. *Neurobiology of Aging, 28*(3), 459-476.

Madden, D. J., Whiting, W. L., Cabeza, R., & Huettel, S. A. (2004). Age-related preservation of top-down attentional guidance during visual search. *Psychology and Aging, 19*(2), 304.

Magliero, A., Bashore, T. R., Coles, M. G., & Donchin, E. (1984). On the dependence of P300 latency on stimulus evaluation processes. *Psychophysiology, 21*(2), 171-186.

Mantini, D., Corbetta, M., Perrucci, M. G., Romani, G. L., & Del Gratta, C. (2009). Large-scale brain networks account for sustained and transient activity during target detection. *NeuroImage, 44*(1), 265-274.

Mattson, M. P., & Arumugam, T. V. (2018). Hallmarks of brain aging: Adaptive and pathological modification by metabolic states. *Cell Metabolism, 27*(6), 1176-1199.

Michel, C. M., & Koenig, T. (2018). EEG microstates as a tool for studying the temporal dynamics of whole-brain neuronal networks: A review. *NeuroImage, 180*, 577-593.

Misiti, M., Misiti, Y., Oppenheim, G., & Poggi, J. (2007). Wavelet toolbox 4–User's guide the MathWorks. *Inc., Massachusetts, USA,*

Mulert, C., Pogarell, O., Juckel, G., Rujescu, D., Giegling, I., Rupp, D., . . . Möller, H. J. (2004). The neural basis of the P300 potential. *European Archives of Psychiatry and Clinical Neuroscience, 254*(3), 190-198.

Mullen, T. R., Kothe, C. A., Chi, Y. M., Ojeda, A., Kerth, T., Makeig, S., . . . Cauwenberghs, G. (2015). Real-time neuroimaging and cognitive monitoring using wearable dry EEG. *IEEE Transactions on Biomedical Engineering, 62*(11), 2553-2567.

Murray, J. D., Demirtaş, M., & Anticevic, A. (2018). Biophysical modeling of large-scale brain dynamics and applications for computational psychiatry. *Biological Psychiatry: Cognitive Neuroscience and Neuroimaging, 3*(9), 777-787.

Nieuwenhuis, S., Aston-Jones, G., & Cohen, J. D. (2005). Decision making, the P3, and the locus coeruleus--norepinephrine system. *Psychological Bulletin, 131*(4), 510.

O'Sullivan, M., Jones, D. K., Summers, P. E., Morris, R. G., Williams, S., & Markus, H. S. (2001). Evidence for cortical "disconnection" as a mechanism of age-related cognitive decline. *Neurology, 57*(4), 632-638.

O'Connell, R. G., Balsters, J. H., Kilcullen, S. M., Campbell, W., Bokde, A. W., Lai, R., . . . Robertson, I. H. (2012). A simultaneous ERP/fMRI investigation of the P300 aging effect. *Neurobiology of Aging, 33*(10), 2448-2461.

Olga, B. (2012). Comments for current interpretation EEG alpha activity: A review and analysis. *Journal of Behavioral and Brain Science, 2012*

Onoda, K., Ishihara, M., & Yamaguchi, S. (2012). Decreased functional connectivity by aging is associated with cognitive decline. *Journal of Cognitive Neuroscience, 24*(11), 2186-2198.

Onoda, K., & Yamaguchi, S. (2013). Small-worldness and modularity of the resting-state functional brain network decrease with aging. *Neuroscience Letters, 556*, 104-108.

Oostenveld, R., Fries, P., Maris, E., & Schoffelen, J. (2011). FieldTrip: Open source software for advanced analysis of MEG, EEG, and invasive electrophysiological data. *Computational Intelligence and Neuroscience, 2011*, 1-9.

Pakkenberg, B., & Gundersen, H. J. G. (1997). Neocortical neuron number in humans: Effect of sex and age. *Journal of Comparative Neurology, 384*(2), 312-320.

Palmer, C., Zapparoli, L., & Kilner, J. M. (2016). A new framework to explain sensorimotor beta oscillations. *Trends in Cognitive Sciences, 20*(5), 321-323.

Palmer, J. A., Kreutz-Delgado, K., & Makeig, S. (2012). AMICA: An adaptive mixture of independent component analyzers with shared components. *Swartz Center for Computatonal Neursoscience, University of California San Diego, Tech.Rep,*

Parks, E. L., & Madden, D. J. (2013). Brain connectivity and visual attention. *Brain Connectivity, 3*(4), 317-338.

Parvizi, J., & Kastner, S. (2018). Human intracranial EEG: Promises and limitations. *Nature Neuroscience, 21*(4), 474.

Pashler, H., Johnston, J. C., & Ruthruff, E. (2001). Attention and performance. *Annual Review of Psychology, 52*(1), 629-651.

Perrin, F., Bertrand, O., & Pernier, J. (1987). Scalp current density mapping: Value and estimation from potential data. *IEEE Transactions on Biomedical Engineering,* (4), 283-288.

Peters, R. (2006). Ageing and the brain. *Postgraduate Medical Journal, 82*(964), 84-88.

Pfefferbaum, A., Sullivan, E. V., Hedehus, M., Lim, K. O., Adalsteinsson, E., & Moseley, M. (2000). Age-related decline in brain white matter anisotropy measured with spatially corrected echo-planar diffusion tensor imaging. *Magnetic Resonance in Medicine: An Official Journal of the International Society for Magnetic Resonance in Medicine, 44*(2), 259-268.

Polich, J. (1996). Meta-analysis of P300 normative aging studies. *Psychophysiology, 33*(4), 334-353.

Polich, J. (1997). EEG and ERP assessment of normal aging. *Electroencephalography and Clinical Neurophysiology/Evoked Potentials Section, 104*(3), 244-256.

Polich, J. (2003). Theoretical overview of P3a and P3b. *Detection of Change,* , 83-98.

Polich, J. (2007). Updating P300: An integrative theory of P3a and P3b. *Clinical Neurophysiology, 118*(10), 2128-2148.

Polich, J., & Bondurant, T. (1997). P300 sequence effects, probability, and interstimulus interval. *Physiology & Behavior, 61*(6), 843-849.

Polich, J., & Criado, J. R. (2006). Neuropsychology and neuropharmacology of P3a and P3b. *International Journal of Psychophysiology, 60*(2), 172-185.

Polich, J., Pollock, V. E., & Bloom, F. E. (1994). Meta-analysis of P300 amplitude from males at risk for alcoholism. *Psychological Bulletin, 115*(1), 55.

Polich, J., & Squire, L. R. (1993). P300 from amnesic patients with bilateral hippocampal lesions. *Electroencephalography and Clinical Neurophysiology, 86*(6), 408-417.

Posner, M. I., & Petersen, S. E. (1990). The attention system of the human brain. *Annual Review of Neuroscience, 13*(1), 25-42.

Raichle, M. E. (2010). Two views of brain function. *Trends in Cognitive Sciences, 14*(4), 180-190.

Raz, N. (2000). Aging of the brain and its impact on cognitive performance: Integration of structural and functional findings.

Raz, N., Lindenberger, U., Rodrigue, K. M., Kennedy, K. M., Head, D., Williamson, A., . . . Acker, J. D. (2005). Regional brain changes in aging healthy adults: General trends, individual differences and modifiers. *Cerebral Cortex, 15*(11), 1676-1689.

Resnick, S. M., Pham, D. L., Kraut, M. A., Zonderman, A. B., & Davatzikos, C. (2003). Longitudinal magnetic resonance imaging studies of older adults: A shrinking brain. *Journal of Neuroscience, 23*(8), 3295-3301.

Richardson, C., Bucks, R. S., & Hogan, A. M. (2011). Effects of aging on habituation to novelty: An ERP study. *International Journal of Psychophysiology, 79*(2), 97-105.

Ridderinkhof, K. R., & Krugers, H. J. (2022). Horizons in human aging neuroscience: From normal neural aging to mental (fr) agility. *Frontiers in Human Neuroscience, 16*, 815759.

Riekmann, A., & Nyberg, L. (2020). Cognitive aging: The role of neurotransmitter systems. *Handbook of Cognitive Aging: A Life Course Perspective,* , 82-100.

Riis, J. L., Chong, H., Ryan, K. K., Wolk, D. A., Rentz, D. M., Holcomb, P. J., & Daffner, K. R. (2008). Compensatory neural activity distinguishes different patterns of normal cognitive aging. *NeuroImage, 39*(1), 441-454.

Rojas, G. M., Alvarez, C., Montoya, C. E., de la Iglesia-Vayá, M., Cisternas, J. E., & Gálvez, M. (2018). Study of resting-state functional connectivity networks using EEG electrodes position as seed. *Frontiers in Neuroscience, 12*, 235.

Rorden, C., & Karnath, H. (2004). Using human brain lesions to infer function: A relic from a past era in the fMRI age? *Nature Reviews Neuroscience, 5*(10), 812-819.

Rossini, P. M., Rossi, S., Babiloni, C., & Polich, J. (2007). Clinical neurophysiology of aging brain: From normal aging to neurodegeneration. *Progress in Neurobiology, 83*(6), 375-400.

Rowe, G., Valderrama, S., Hasher, L., & Lenartowicz, A. (2006). Attentional disregulation: A benefit for implicit memory. *Psychology and Aging, 21*(4), 826.

Rubinov, M., & Sporns, O. (2010). Complex network measures of brain connectivity: Uses and interpretations. *NeuroImage, 52*(3), 1059-1069.

Rugg, M. D., Pickles, C. D., Potter, D. D., & Roberts, R. C. (1991). Normal P300 following extensive damage to the left medial temporal lobe. *Journal of Neurology, Neurosurgery & Psychiatry, 54*(3), 217-222.

Salthouse, T. A. (2000). Aging and measures of processing speed. *Biological Psychology, 54*(1-3), 35-54.

Samar, V. J., Bopardikar, A., Rao, R., & Swartz, K. (1999). Wavelet analysis of neuroelectric waveforms: A conceptual tutorial. *Brain and Language, 66*(1), 7-60.

Samar, V. J., Swartz, K. P., & Raghuveer, M. R. (1995). Multiresolution analysis of event-related potentials by wavelet decomposition. *Brain and Cognition, 27*(3), 398-438.

Sawaki, R., & Katayama, J. (2008). Distractor P3 is associated with attentional capture by stimulus deviance. *Clinical Neurophysiology, 119*(6), 1300-1309.

Schmidt, R., Ruiz, M. H., Kilavik, B. E., Lundqvist, M., Starr, P. A., & Aron, A. R. (2019). Beta oscillations in working memory, executive control of movement and thought, and sensorimotor function. *Journal of Neuroscience, 39*(42), 8231-8238.

Schmitz, T. W., Cheng, F. H., & De Rosa, E. (2010). Failing to ignore: Paradoxical neural effects of perceptual load on early attentional selection in normal aging. *Journal of Neuroscience, 30*(44), 14750-14758.

Schöbi, D., Do, C., Frässle, S., Tittgemeyer, M., Heinzle, J., & Stephan, K. E. (2021). A fast and robust integrator of delay differential equations in DCM for electrophysiological data. *NeuroImage, 244*, 118567.

Schürmann, M., & Başar, E. (2001). Functional aspects of alpha oscillations in the EEG. *International Journal of Psychophysiology, 39*(2-3), 151-158.

Schurr, R., Zelman, A., & Mezer, A. A. (2020). Subdividing the superior longitudinal fasciculus using local quantitative MRI. *NeuroImage, 208*, 116439.

Sciberras-Lim, E. T., & Lambert, A. J. (2017). Attentional orienting and dorsal visual stream decline: Review of behavioral and EEG studies. *Frontiers in Aging Neuroscience, 9*, 246.

Serences, J. T., Schwarzbach, J., Courtney, S. M., Golay, X., & Yantis, S. (2004). Control of object-based attention in human cortex. *Cerebral Cortex, 14*(12), 1346-1357.

Shafiei, G., Zeighami, Y., Clark, C. A., Coull, J. T., Nagano-Saito, A., Leyton, M., . . . Mišić, B. (2019). Dopamine signaling modulates the stability and integration of intrinsic brain networks. *Cerebral Cortex, 29*(1), 397-409.

Shallice, T., Mussoni, A., D'Agostino, S., & Skrap, M. (2010). Right posterior cortical functions in a tumour patient series. *Cortex, 46*(9), 1178-1188.

Shaw, E. E., Schultz, A. P., Sperling, R. A., & Hedden, T. (2015). Functional connectivity in multiple cortical networks is associated with performance across cognitive domains in older adults. *Brain Connectivity, 5*(8), 505-516.

Shettigar, N., Yang, C., Tu, K., & Suh, C. S. (2022). On the biophysical complexity of brain dynamics: An outlook. *Dynamics, 2*(2), 114-148.

Shulman, G. L., Astafiev, S. V., McAvoy, M. P., d'Avossa, G., & Corbetta, M. (2007). Right TPJ deactivation during visual search: Functional significance and support for a filter hypothesis. *Cerebral Cortex, 17*(11), 2625-2633.

Smith, M. E., Halgren, E., Sokolik, M., Baudena, P., Musolino, A., Liegeois-Chauvel, C., & Chauvel, P. (1990). The intracranial topography of the P3 event-related potential elicited during auditory oddball. *Electroencephalography and Clinical Neurophysiology, 76*(3), 235-248.

Solbakk, A., Alpert, G. F., Furst, A. J., Hale, L. A., Oga, T., Chetty, S., . . . Knight, R. T. (2008). Altered prefrontal function with aging: Insights into age-associated performance decline. *Brain Research, 1232*, 30-47.

Spencer, K. M., Dien, J., & Donchin, E. (1999). A componential analysis of the ERP elicited by novel events using a dense electrode array. *Psychophysiology, 36*(3), 409-414.

Spencer, K. M., Dien, J., & Donchin, E. (2001). Spatiotemporal analysis of the late ERP responses to deviant stimuli. *Psychophysiology, 38*(2), 343-358.

Spitzer, B., & Haegens, S. (2017). Beyond the status quo: A role for beta oscillations in endogenous content (re) activation. *Eneuro, 4*(4)

Sporns, O., & Honey, C. J. (2006). Small worlds inside big brains. *Proceedings of the National Academy of Sciences, 103*(51), 19219-19220.

Squires, K. C., Donchin, E., Herning, R. I., & McCarthy, G. (1977). On the influence of task relevance and stimulus probability on event-related-potential components. *Electroencephalography and Clinical Neurophysiology, 42*(1), 1-14.

Stanley, M. L., Simpson, S. L., Dagenbach, D., Lyday, R. G., Burdette, J. H., & Laurienti, P. J. (2015). Changes in brain network efficiency and working memory performance in aging. *PLoS One, 10*(4), e0123950.

Strobel, A., Debener, S., Sorger, B., Peters, J. C., Kranczioch, C., Hoechstetter, K., . . . Goebel, R. (2008). Novelty and target processing during an auditory novelty oddball: A simultaneous event-related potential and functional magnetic resonance imaging study. *NeuroImage, 40*(2), 869-883.

Sutton, S., Braren, M., Zubin, J., & John, E. R. (1965). Evoked-potential correlates of stimulus uncertainty. *Science, 150*(3700), 1187-1188.

Tang, Y., Rothbart, M. K., & Posner, M. I. (2012). Neural correlates of establishing, maintaining, and switching brain states. *Trends in Cognitive Sciences, 16*(6), 330-337.

Tian, L., Li, Q., Wang, C., & Yu, J. (2018). Changes in dynamic functional connections with aging. *NeuroImage, 172*, 31-39.

Tononi, G., Sporns, O., & Edelman, G. M. (1994). A measure for brain complexity: Relating functional segregation and integration in the nervous system. *Proceedings of the National Academy of Sciences, 91*(11), 5033-5037.

Tucker, D. M. (1993). Spatial sampling of head electrical fields: The geodesic sensor net. *Electroencephalography and Clinical Neurophysiology, 87*(3), 154-163.

Tucker, D. M., Liotti, M., Potts, G. F., Russell, G. S., & Posner, M. I. (1994). Spatiotemporal analysis of brain electrical fields. *Human Brain Mapping, 1*(2), 134-152.

Unser, M., Aldroubi, A., & Eden, M. (1992). On the asymptotic convergence of B-spline wavelets to gabor functions. *IEEE Transactions on Information Theory, 38*(2), 864-872.

Vaidya, A. R., Pujara, M. S., Petrides, M., Murray, E. A., & Fellows, L. K. (2019). Lesion studies in contemporary neuroscience. *Trends in Cognitive Sciences, 23*(8), 653-671.

Vallesi, A., Stuss, D. T., McIntosh, A. R., & Picton, T. W. (2009). Age-related differences in processing irrelevant information: Evidence from event-related potentials. *Neuropsychologia, 47*(2), 577-586.

Van Diessen, E., Numan, T., Van Dellen, E., Van Der Kooi, A. W., Boersma, M., Hofman, D., . . . Hillebrand, A. (2015). Opportunities and methodological challenges in EEG and MEG resting state functional brain network research. *Clinical Neurophysiology, 126*(8), 1468-1481.

Verheyden, G., Nieuwboer, A., De Wit, L., Thijs, V., Dobbelaere, J., Devos, H., . . . De Weerdt, W. (2008). Time course of trunk, arm, leg, and functional recovery after ischemic stroke. *Neurorehabilitation and Neural Repair, 22*(2), 173-179.

Verleger, R. (1988). Event-related potentials and cognition: A critique of the context updating hypothesis and an alternative interpretation of P3. *Behavioral and Brain Sciences, 11*(3), 343-356.

Verleger, R. (2008). P3b: Towards some decision about memory. *Clinical Neurophysiology, 4*(119), 968-970.

Verleger, R., Neukäter, W., Kömpf, D., & Vieregge, P. (1991). On the reasons for the delay of P3 latency in healthy elderly subjects. *Electroencephalography and Clinical Neurophysiology, 79*(6), 488-502.

Viviano, R. P., Raz, N., Yuan, P., & Damoiseaux, J. S. (2017). Associations between dynamic functional connectivity and age, metabolic risk, and cognitive performance. *Neurobiology of Aging, 59*, 135-143.

Volkow, N. D., Logan, J., Fowler, J. S., Wang, G., Gur, R. C., Wong, C., . . . Hitzemann, R. (2000). Association between age-related decline in brain dopamine activity and impairment in frontal and cingulate metabolism. *American Journal of Psychiatry, 157*(1), 75-80.

Volpe, U., Mucci, A., Bucci, P., Merlotti, E., Galderisi, S., & Maj, M. (2007). The cortical generators of P3a and P3b: A LORETA study. *Brain Research Bulletin, 73*(4-6), 220-230.

Vossel, S., Geng, J. J., & Fink, G. R. (2014). Dorsal and ventral attention systems: Distinct neural circuits but collaborative roles. *The Neuroscientist, 20*(2), 150-159.

Vossel, S., Weidner, R., Driver, J., Friston, K. J., & Fink, G. R. (2012). Deconstructing the architecture of dorsal and ventral attention systems with dynamic causal modeling. *Journal of Neuroscience, 32*(31), 10637-10648.

Walhovd, K. B., & Fjell, A. M. (2003). The relationship between P3 and neuropsychological function in an adult life span sample. *Biological Psychology, 62*(1), 65-87.

Walhovd, K. B., Rosquist, H., & Fjell, A. M. (2008). P300 amplitude age reductions are not caused by latency jitter. *Psychophysiology, 45*(4), 545-553.

Wang, C., Ulbert, I., Schomer, D. L., Marinkovic, K., & Halgren, E. (2005). Responses of human anterior cingulate cortex microdomains to error detection, conflict

monitoring, stimulus-response mapping, familiarity, and orienting. *Journal of Neuroscience, 25*(3), 604-613.

Warren, C. V., Kroll, C. F., & Kopp, B. (2023). Dopaminergic and norepinephrinergic modulation of endogenous event-related potentials: A systematic review and meta-analysis. *Neuroscience & Biobehavioral Reviews,* , 105221.

Watts, D. J., & Strogatz, S. H. (1998). Collective dynamics of 'small-world'networks. *Nature, 393*(6684), 440-442.

Wen, X., Yao, L., Liu, Y., & Ding, M. (2012). Causal interactions in attention networks predict behavioral performance. *Journal of Neuroscience, 32*(4), 1284-1292.

West, R., Schwarb, H., & Johnson, B. N. (2010). The influence of age and individual differences in executive function on stimulus processing in the oddball task. *Cortex, 46*(4), 550-563.

Wieloch, T., & Nikolich, K. (2006). Mechanisms of neural plasticity following brain injury. *Current Opinion in Neurobiology, 16*(3), 258-264.

Winkler, I., Haufe, S., & Tangermann, M. (2011). Automatic classification of artifactual ICA-components for artifact removal in EEG signals. *Behavioral and Brain Functions, 7*(1), 1-15.

Wood, C. C., & McCarthy, G. (1985). A possible frontal lobe contribution to scalp P300. Paper presented at the *Neuroscience Abstracts, , 11* 879.

Woodman, G. F. (2010). A brief introduction to the use of event-related potentials in studies of perception and attention. *Attention, Perception, & Psychophysics, 72*(8), 2031-2046.

Yamazaki, T., Kamijo, K., Kiyuna, T., Takaki, Y., & Kuroiwa, Y. (2001). Multiple dipole analysis of visual event-related potentials during oddball paradigm with silent counting. *Brain Topography, 13*(3), 161-168.

Yordanova, J., Devrim, M., Kolev, V., Ademoglu, A., & Demiralp, T. (2000). Multiple time-frequency components account for the complex functional reactivity of P300. *Neuroreport, 11*(5), 1097-1103.

Zeidman, P., Jafarian, A., Seghier, M. L., Litvak, V., Cagnan, H., Price, C. J., & Friston, K. J. (2019). A guide to group effective connectivity analysis, part 2: Second level analysis with PEB. *NeuroImage, 200*, 12-25.